AD NUMBER

ADB202855

NEW LIMITATION CHANGE

TO

Approved for public release, distribution unlimited

FROM

Distribution authorized to U.S. Gov't. agencies and their contractors; Administrative/Operational Use; DEC 1949. Other requests shall be referred to Ballistic Research Laboratories, Aberdeen Proving Ground, MD.

AUTHORITY

BRL ltr dtd 22 Apr 1981

BALLISTIC RESEARCH LABORATORIES

REPORT NO. 711

A Method of Determining Some Aerodynamic Coefficients from Supersonic Free Flight Tests of a Rolling Missile

RAY E. BOLZ
JOHN D. NICOLAIDES

ABERDEEN PROVING GROUND, MARYLAND

BALLISTIC RESEARCH LABORATORIES

REPORT NO. 711

A Method of Determining Some Aerodynamic Coefficients from Supersonic Free Flight Tests of a Rolling Missile

RAY E. BOLZ
JOHN D. NICOLAIDES

DECEMBER 1949

Part of the material presented in this paper appeared as the experimental portion of a Doctoral Dissertation for Yale University (June 1949) by R. E. Bolz, Assistant Professor, Rensselaer Polytechnic Institute.

ABERDEEN PROVING GROUND, MARYLAND

CONTENTS

BALLISTIC RESEARCH LABORATORIES

REPORT NO. 711

Ray E. Bolz/John D. Nicolaides
Aberdeen Proving Ground, Md.
14 November 1949

A METHOD OF DETERMINING SOME AERODYNAMIC COEFFICIENTS FROM SUPERSONIC FREE FLIGHT TESTS OF A ROLLING MISSILE

ABSTRACT

Based on the assumption that the aerodynamic forces acting at any point on a lifting surface are linearly dependent upon the local angle of attack at that point, the theory of pure rolling motion is applied to the experimentally observed motion of a finned missile in order to

1. determine how well the actual motion is represented by the theory,
2. determine the suitability of the Aerodynamic Range to the proposed free-flight roll technique, and
3. determine certain aerodynamic coefficients associated with the motion.

Values for the aerodynamic coefficients are also derived using the linearized supersonic theory and are compared with those obtained from experiment.

The results indicate that the actual motion is well represented by the theory to within the small experimental errors and that excellent reproducibility of the aerodynamic coefficients in roll is obtained. Furthermore the results show a fairly good correlation with the linearized theory considering the degree of approximation associated with this theory when applied to aerodynamic surfaces of 16% thickness as employed on the missiles used in the reported tests.

SYMBOLS AND COEFFICIENTS

a	radius of body of missile
A_p	area of fin or wing panel (see Figure 1)
A,B	arbitrary constants depending on boundary conditions
b	wing span
B	$\sqrt{M^2 - 1}$
c	wing chord
C_1	damping constant $\left(\frac{K_{\ell_p}}{I} - \frac{K_R}{M}\right)$
C_2	$\frac{K_{\ell_\delta}}{I}$
C_D	drag coefficient
C_{ℓ_δ}	roll moment derivative due to canted surface $\left(\frac{\partial C_\ell}{\partial \delta}\right)$, δ in rad.
C_{ℓ_p}	roll moment derivative due to rolling velocity, $\frac{\partial C_\ell}{\partial (\frac{pb}{2V})}$
C_ℓ	roll moment coefficient, $\frac{L}{qA_p b}$
d	diameter of body
$\left(\frac{dC_L}{d\alpha}\right)_{x,y}$	slope of the lift curve at any point x,y on fin
K_{ℓ_δ}	L_δ / V^2
K_{ℓ_p}	L_p / pV
K_R	$\frac{\rho}{2} SC_D$
L_δ	rolling moment due to angle of cant
L_p	rolling moment due to rolling velocity, damping moment
I	axial moment of inertia (slugs - ft^2)
M	Mach number
m	mass (slugs)
n_δ	number of canted fins
n	total number of fins
p	rolling velocity ($\dot{\phi}$), rad/sec

p_s	steady state rolling velocity $(\dot{\phi})_\infty$, $\frac{rad}{sec}$
P.E.	probable error
$\frac{pb}{2V}$	fin tip helix angle
$\frac{p_s b}{2V}$	steady-state fin tip helix angle
S	$\frac{\pi}{4} d^2$
s	steady state rolling velocity (°/ft)
V	linear velocity of missile along trajectory, ft/sec
x,y	Cartesian coordinates, y along fin span, x along fin chord
z	linear distance along the free-flight range
α	angle of attack
δ	angle of cant on one fin
β	tip mach cone angle
μ ,r	polar coordinates shown in figure 3
ρ	free stream air density, $\frac{slugs}{ft^3}$
ϕ	angle of roll
Ω	$s - \phi'$

Superscripts

"dot" over symbol is time derivative of variable

"prime" mark above symbol is the derivative with respect to Z, distance along range.

INTRODUCTION

A continually guided supersonic missile is possible only after roll control has been obtained, and the difficulties in achieving this are well known. The design of a reliable roll stabilization system requires an accurate knowledge of the dynamic as well as the static aerodynamic coefficients associated with the rolling motion. Since the Aerodynamic Range appeared to offer promise as a new tool for the determination of both static and dynamic coefficients associated with aerodynamic configurations, an attempt to determine these critical rolling coefficients seemed to be a valuable initial undertaking. Some of the ballistic contributions to aerodynamics, as determined in the Aerodynamic Range are presented by Charters[1], and a detailed description of the Range is given by Charters and Thomas[2].

In this preliminary report the theory of pure rolling motion is applied to the experimentally observed motion in order to obtain the aerodynamic coefficients associated with the motion. The fit of the equation of rolling motion to the range data is obtained, and a comparison is made of the experimentally obtained aerodynamic coefficients to those predicted by a linearized theory.

It is not intended that this paper present the results of a finished research program, but rather to discuss the basic theory of motion, the general test procedure, the method of data reduction, some specific results from the experimental technique, and the experimental accuracy that is attained.

GENERAL EXPERIMENTAL TECHNIQUE

A suitable aerodynamic test vehicle is gun-launched down the Aerodynamic Free-Flight Range. The special firing technique employed, results in very small pitching and yawing displacements of the test vehicle during the subsequent flight. This vehicle may be a model of any aerodynamically stable missile configuration having one or more pairs of fins set at a differential angle of incidence (cant) to induce a rolling velocity. During flight, as it passes each of twenty-five stations accurately located to 0.001 feet along a 218-foot distance, the missile is photographed (shadowgraphs) simultaneously in the vertical and horizontal planes by means of an extremely short-duration spark discharge. The time of occurrance of the discharge for 9 of the stations is measured to within 10^{-6} seconds. From the photographs, the spatial orientation of the missile is obtained, from which the linear displacements (to 0.001 ft. accuracy) and angular displacements in roll (to $\pm$.7 degree accuracy) are determined at the 25 discrete distances along the trajectory, as well as at 9 discrete values of time.

With these data obtained from the Aerodynamic Range and the analyses in the following sections, the aerodynamic coefficients associated with the rolling motion may be determined and compared with the theoretical values calculated on the basis of linearized supersonic theory.

---

1 - "Some Ballistic Contributions to Aerodynamics", A. C. Charters, Journal of the Aeronautical Sciences, Vol. 14, No. 3, p. 155, March 1947.

2 - "The Aerodynamic Performance of Small Spheres from Subsonic to High Supersonic Velocities", A. C. Charters and R. N. Thomas, Journal of the Aeronautical Sciences, Vol. 12, No. 4, p. 468, October 1945.

THEORY

A. Equation of Motion of a Missile in Pure Roll.

If a symmetrical winged and/or finned missile with canted surfaces is in free flight and has an angular motion of pure roll (yawing and pitching displacements negligible), the missile may be considered as being acted upon by two roll moments. One moment, tending to increase the roll velocity, results from the lift-force couple produced by the canted surfaces in linear forward motion and the second moment, tending to decrease the roll velocity, is the damping moment produced by the lift-force couples induced on all the aerodynamic surfaces by the roll velocity itself.

1. Roll Moment of a Missile Due to Canted Fins.

The roll moment induced by n_δ differentially offset (canted) wing or tail panels, may be expressed as the integrated product of the aerodynamic lift force and the moment arm of this force about the missile axis. A double integration is convenient because a finite wing moving through air at supersonic velocities experiences a variable pressure over the surface within the region bounded by the wing-tip Mach cone. Consequently, from Figure 1 the roll moment may be written as:

$$L_\delta = n_\delta \int_{x=0}^{c} \int_{y=a}^{b/2} \left(\frac{dC_L}{d\alpha}\right)_{x,y} \delta \frac{\rho V^2}{2} \, ydxdy \tag{1}$$

where $\left(\frac{dC_L}{d\alpha}\right)_{x,y}$ = slope of the lift curve at any point x,y

n_δ = number of identical, canted wing or tail panels on the missile

δ = angle of cant

Then

$$\text{a)} \quad L_\delta = \frac{n_\delta \rho V^2}{2} \int_{x=0}^{c} \int_{y=a}^{b/2} \left(\frac{dC_L}{d\alpha}\right)_{x,y} \delta \, ydxdy$$

$$\text{b)} \quad L_\delta = K_{\ell_\delta} V^2 \tag{2}$$

2. Roll Moment Due to Rolling Velocity - Damping Moment. When a missile rolls about its own axis, the lifting surfaces are subjected to a normal velocity vector induced by the rolling velocity. The induced velocity results in an induced angle of attack on the surface which varies over the surface as a linear function of the radial distance from the rotational axis. If the roll damping moment, neglecting the viscous damping on the fuselage, [1] is defined as the roll moment induced by and opposing or damping the rolling velocity, then

[1] The effect of viscous damping of a missile fuselage may be estimated from the performance of spinning bodies of revolution as determined in the Aerodynamic Range. The numerical value of the viscous damping coefficient of our missile is approximately 0.16% of the aerodynamic damping coefficient obtained due to the fins. Consequently the effect of body damping may then be neglected for the purposes of this report.

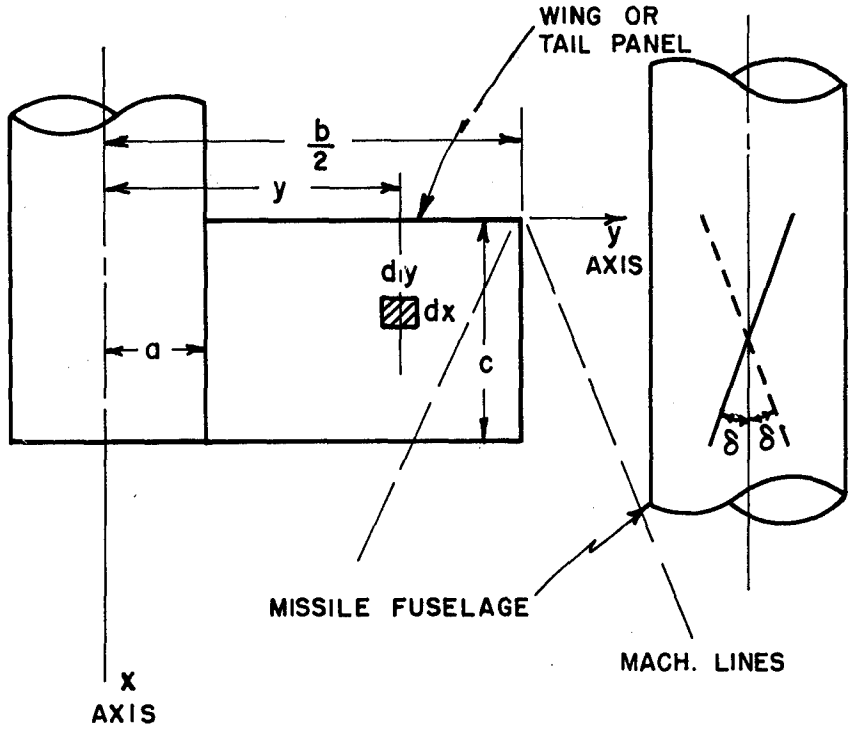

FIGURE 1 - SCHEMATIC OF A MISSILE WING OR TAIL PANEL.

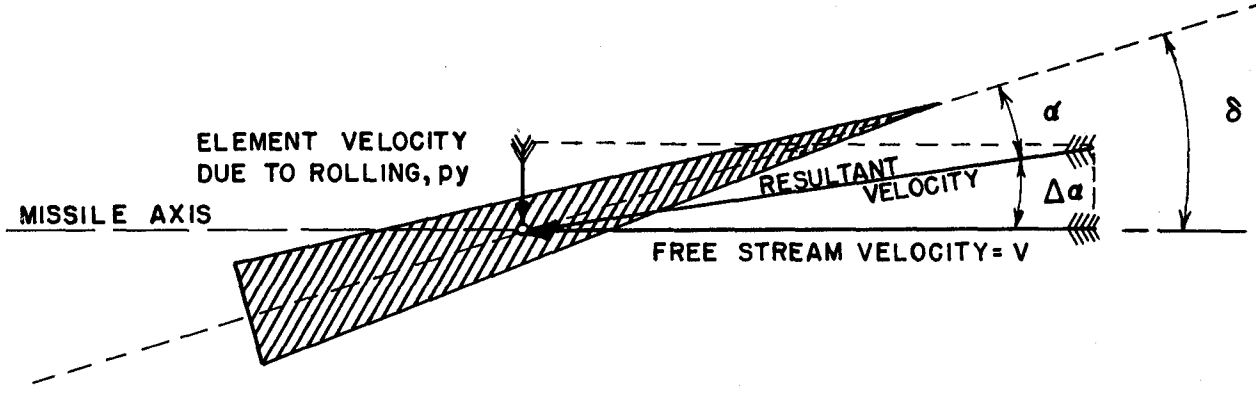

$$\Delta\alpha = \frac{py}{V}$$

FIGURE 2: SCHEMATIC SHOWING ANGLE OF ATTACK OF ANY ELEMENT OF A ROLLING SURFACE FOR PURE ROLLING MOTION.

this aerodynamic damping moment (with reference to Figures 1 and 2) may be expressed by a double integration as follows:

$$L_p = n \int_{x=0}^{c} \int_{y=a}^{b/2} \left(\frac{dC_L}{d\alpha}\right)_{x,y} \frac{py}{V} \frac{\rho V^2}{2} \, y \, dx \, dy \qquad (3)$$

where $\frac{py}{V}$ is the induced angle of attack on the lifting surfaces, and n is the number of identical wing or tail panels (see Figure 1) mounted on the missile fuselage.

$$a) \quad L_p = pV \frac{\rho n}{2} \int_{x=0}^{c} \int_{y=a}^{b/2} \left(\frac{dC_L}{d\alpha}\right)_{x,y} y^2 \, dx \, dy \qquad (4)$$

$$b) \quad L_p = K_{\ell_p} pV \qquad (4)$$

3. Dynamical Equation of Roll. Applied to a symmetrical missile in pure rolling flight, subject to small pitching and yawing displacements, the dynamical equation in roll becomes simply:

$$I\ddot{\phi} = L_\delta - L_p \qquad (5)$$

Here the rolling moments exerted by the wing and tail surfaces arising from the pitching and yawing angular displacements and angular velocities have been neglected because (1) for small pitching and yawing displacements (mean square yaw less than 1.5°) these moments are extremely small and of second order compared with L_δ and L_p (see Appendix A) and (2) they are oscillatory with respect to their direction of action and as such any small effect that they may otherwise exert on the resulting rolling motion tends to cancel out.

B. Solution of Dynamical Equation of Roll.

For the missiles traveling the length of the range between stations (218 feet), the decrease in velocity is less than 7 percent and for values of flight Mach number in excess of 1.6 the variation of $dC_L/d\alpha$, the slope of the lift curve, resulting from this small deceleration is less than about 3.5 percent from the average value. Therefore little error is introduced if the values of K_{ℓ_p} and K_{ℓ_δ} in equations (2) and (4) are considered as constant for any given flight.

Insertion of equations (2) and (4) into (5) gives:

$$I\ddot{\phi} + K_{\ell_p} \dot{\phi} V = K_{\ell_\delta} V^2 \qquad (6)$$

where

$$K_{\ell_\delta} = \frac{\rho n_\delta}{2} \int_{x=0}^{c} \int_{y=a}^{b/2} \left(\frac{dC_L}{d\alpha}\right)_{x,y} \delta y \, dx \, dy \qquad (7)$$

$$K_{\ell_p} = \frac{\rho n}{2} \int_0^c \int_{y=a}^{b/2} \left(\frac{dC_L}{d\alpha}\right)_{x,y} y^2 \, dx \, dy \tag{8}$$

and $\dot{\phi} = \frac{d\phi}{dt} = p$ the rolling velocity.

The approximate linear equation of motion of the missile along the trajectory may be written:

$$m\dot{V} = -K_R V^2 \tag{9a}$$

where

$$K_R = \frac{\rho}{2} S C_D \tag{9b}$$

is considered constant for the small variation in velocity V.

Equations (6) and (9) are now transformed to the independent variable, z, the distance along the trajectory, [1] by:

$$\frac{d}{dt} = \frac{dz}{dt}\frac{d}{dz} = V\frac{d}{dz} \tag{10}$$

$$\frac{d^2}{dt^2} = V^2 \frac{d^2}{dz^2} + V\frac{dv}{dz}\frac{d}{dz}$$

If a prime is used to denote a derivative with respect to z, then equations (6) and (9) become:

$$\phi'' + \phi'\left(\frac{V'}{V} + \frac{K_{\ell_p}}{I}\right) - \frac{K_{\ell_\delta}}{I} = 0 \tag{11}$$

and

$$\frac{V'}{V} = -\frac{K_R}{m} \tag{12}$$

Substitution of (12) into (11) gives:

$$\phi'' + \phi'\left(\frac{K_{\ell_p}}{I} - \frac{K_R}{m}\right) - \frac{K_{\ell_\delta}}{I} = 0$$

a linear differential equation with constant coefficients.

---

[1] In the Range, the distance along the trajectory may be assumed equal to the distance along the range with negligible error, and the vector velocity

$$V = \frac{dz}{dt} + \frac{dx}{dt} + \frac{dy}{dt}$$

where

$$\frac{dx}{dt} \text{ and } \frac{dy}{dt} << \frac{dz}{dt}$$

becomes

$$V = \frac{dz}{dt} \text{ with negligible error.}$$

Defining

$$C_1 = \frac{K_{\ell_p}}{I} - \frac{K_R}{m} \tag{13a}$$

$$C_2 = \frac{K_{\ell_\delta}}{I} \tag{13b}$$

Equation (12) becomes:

$$\ddot{\phi} + C_1\dot{\phi} - C_2 = 0 \tag{14}$$

The general solution of Equation (14) may be written down immediately as:

$$\phi = B + sz + Ae^{-C_1 z} \tag{15}$$

where

$$s = \frac{C_2}{C_1} \equiv \text{steady-state rolling velocity.} \tag{16}$$

A and B are arbitrary constants which depend upon the boundary conditions written as follows:

For $z = 0$, $\phi = \phi_o$ and $\phi' = \phi'_o$

$z = \infty$, $\phi' = \phi'_\infty$

Then equation (15) becomes;

$$\phi = \phi_o + \phi'_\infty z + \frac{(\phi'_\infty - \phi'_o)}{C_1}\left(e^{-C_1 z} - 1\right) \tag{17}$$

Equation (15) then should represent the form of the curve connecting the set of experimental data points of roll angle versus distance along the trajectory obtained from the firings in the range. A curve of the form given in equation (15) then is fitted to the data points by successive applications of the method of Differential Corrections and the constants C_1 and C_2 as well as K_{ℓ_p} and K_{ℓ_δ} are determined experimentally. Thus the damping and rolling moments can be experimentally determined as a function of missile design and Mach number.

B. Theoretical Determination of the Roll-Moment Coefficients.

The values for K_{ℓ_p} and K_{ℓ_δ} defined in equations (7) and (8) are determined experimentally in the Aerodynamic Range by the technique discussed in this paper. However, approximate values for these two coefficients may also be determined theoretically from the application of the existing linearized supersonic theory.

The theory as applied here assumes the two-dimensional valve of $\left(\frac{dC_L}{d\alpha}\right)$ in the areas of the fins outside the tip region for the calculation of K_{ℓ_p} and K_{ℓ_δ}. This assumption, of course, cannot give the cor-

rect lift distribution on the wing within the Mach cone originating from the intersection of the wing leading edge with the body. Since this region in which the lift distribution is incorrectly calculated is close to the body, the resultant error in the rolling moments should be small.

The effects of body-wing interference when the body is at an angle of yaw have also been neglected. However, in the roll tests in the Aerodynamic Range, it should be noted that the body yaw during flight down the range is always intentionally restricted by the launching technique to a very small angle (mean square yaw less than 1.5°) in order for equation (6) to be very nearly exact. Any upwash on the wing due to body-wing interaction resulting from the yawed body would result in (1) small symmetrical forces (lift forces in the same direction on both halves of the fin) when the fins are oriented at 0 or 45 degrees to the plane of yaw, and (2) possibly very small unsymmetrical forces due to flow dissimilarities when the missile is oriented in roll to any angle other than those stated above referred again to the plane of yaw. Since a roll moment can obviously arise only from the unsymmetrical forces, it may be concluded from the qualitative observations above that any roll moments resulting from body upwash phenomena would not only be very small moments but would be rapidly oscillating both in sign as well as in magnitude. Such moments would contribute negligible effect to the rolling motion of the missile resulting from the relatively large and continuously directed moments, L_p and L_δ .

1. Determination of K_{ℓ_p} from the Linearized Supersonic Theory.

From the linearized two-dimensional theory of Ackeret[1], the value of the lift slope at all points on the surface of an infinite-aspect-ratio lifting surface is given by the expression:

$$\left(\frac{dC_L}{d\alpha}\right)_{x,\,y} = \frac{4}{\sqrt{M^2 - 1}} = \frac{4}{B} \tag{18}$$

which is a function of Mach number only. However, for a finite wing or tail surface, the pressure distribution over the lifting surface included within the tip Mach cone is influenced by the wing-tip boundary conditions as well as by the variable angle of attack ($\frac{py}{V}$ helix angle) induced over the surface by the rolling velocity. This pressure distribution is evaluated on the basis of the three-dimensional linearized supersonic theory[2], using Evvard's[3] method. The value then for $\left(\frac{dC_L}{d\alpha}\right)_{x,\,y}$ for any incremental area on a rectangular wing within the Mach cone boundary is,

$$\left(\frac{dC_L}{d\alpha}\right)_{x,\,y} = \frac{8}{\pi B}\left(\sin^{-1}\sqrt{\frac{B}{x}\left(\frac{b}{2} - y\right)} - \frac{1}{y}\sqrt{\left(\frac{b}{2} - y\right)\left(y - \frac{b}{2} + \frac{x}{B}\right)}\right) \tag{19}$$

a function of position (x, y) on the wing as well as of the flight Mach number.

---

[1] Liepmann, H. W., and Puckett, A. E., Aerodynamics of a Compressible Fluid, Chapter 9, John Wiley and Sons, Incl., 1947.

[2] Harmon, S. M. "Stability Derivatives of Thin Rectangular Wings at Supersonic Speeds", NACA TN No. 1706, November, 1948.

[3] Evvard, J. C., "Distribution of Wave Drag and Lift in the Vicinity of Wing Tips at Supersonic Speeds", NACA TN No. 1382, 1947.

From Figure 3,

$$K_{\ell_p} = \left(K_{\ell_p}\right)_{\text{area I}} + \left(K_{\ell_p}\right)_{\text{area II}} + \left(K_{\ell_p}\right)_{\text{area III}} \tag{20}$$

For Area I

From equations (8) and (19) using dS in place of dx dy for the differential area

$$\left(K_{\ell_p}\right)_I = \frac{\rho n}{2} \int_S \frac{8}{\pi B}\left(\sin^{-1}\sqrt{\frac{B}{x}\left(\frac{b}{2} - y\right)} - \frac{1}{y}\sqrt{\left(\frac{b}{2} - y\right)\left(y - \frac{b}{2} + \frac{x}{B}\right)}\right) y^2 \, dS \tag{21}$$

where from Figure 3,

$$dS = r \, d\mu \, dr = \frac{x}{\cos\mu} \quad \frac{dx}{\cos\mu} \, d\mu \tag{22}$$

Inserting (22) into (21) gives:

$$\left(K_{\ell_p}\right)_I = \frac{4\rho n}{\pi B} \int_{\mu=0}^{\tan^{-1}\left(\frac{1}{B}\right)} \int_{x=0}^{c} \left(y \sin^{-1}\sqrt{\frac{B}{x}\left(\frac{b}{2} - y\right)} - \sqrt{\left(\frac{b}{2} - y\right)\left(y - \frac{b}{2} + \frac{x}{B}\right)}\right) \frac{y \, x \, d\mu \, dx}{\cos^2\mu}$$

From Figure 3,

$$y = \frac{b}{2} - x \tan\mu$$

and

$$\left(K_{\ell_p}\right)_I = \frac{4\rho n}{\pi B} \int_0^{\tan^{-1}\left(\frac{1}{B}\right)} \int_0^{c} \left\{ \frac{x\left(\frac{b}{2} - x\tan\mu\right)^2 \sin^{-1}\sqrt{B\tan\mu} - \left(\frac{b}{2} - x\tan\mu\right) x^2 \sqrt{\frac{\tan\mu}{B} - \tan^2\mu}}{\cos^2\mu} \right\} d\mu \, dx$$

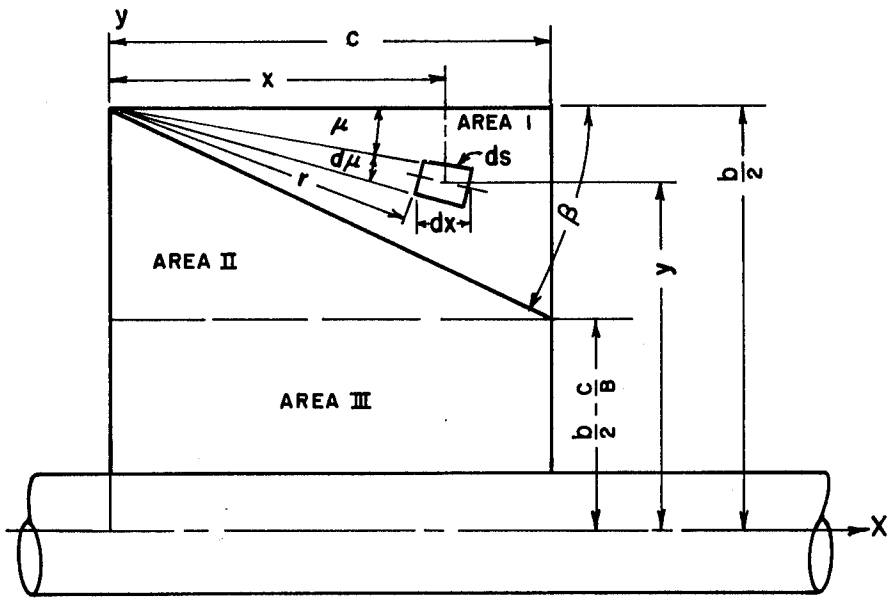

FIGURE 3- SKETCH INDICATING METHOD OF INTEGRATION FOR ROLL MOMENTS.

Integrating for x first and then μ and finally evaluating the limits results in

$$(K_{\ell_p})_I = \frac{4\rho n}{B^2}\left(\frac{c^2b^2}{32} - \frac{7c^3b}{96B} + \frac{17c^4}{384B^2}\right) \tag{23}$$

For Area II:

From Equations (8) and (18)

$$(K_{\ell_p})_{II} = \frac{2\rho n}{B}\int_{x=0}^{B(\frac{b}{2}-y)}\int_{y=(\frac{b}{2}-\frac{c}{B})}^{\frac{b}{2}} y^2\,dx\,dy$$

$$(K_{\ell_p})_{II} = \frac{2\rho n}{B}\left(\frac{c^4}{4B^3} + \frac{c^2b^2}{8B} - \frac{c^3b}{3B^2}\right) \tag{24}$$

For Area III:

From Equations (8) and (18)

$$(K_{\ell_p})_{III} = \frac{\rho n}{2}\int_{a}^{\frac{b}{2}-\frac{c}{B}} \frac{4}{B}\,y^2\,c\,dy$$

$$(K_{\ell_p})_{III} = \frac{2\rho n}{B}\left(\frac{cb^3}{24} - \frac{c^2b^2}{4B} + \frac{c^3b}{2B^2} - \frac{c^4}{3B^3} - \frac{ca^3}{3}\right) \tag{25}$$

and adding Equations (23), (24) and (25) results in

$$K_{\ell_p} = \frac{2\rho n}{B}\left(\frac{c^4}{192B^3} + \frac{c^3b}{48B^2} - \frac{c^2b^2}{16B} + \frac{cb^3}{24} - \frac{ca^3}{3}\right) \tag{26}$$

2. Determination of K_{ℓ_δ} from Linearized Supersonic Theory.

The expression for K_{ℓ_δ} is determined by an integration of Equation (7). Here again Equation (18) gives the value of the lift slope on the wing or tail surface at all points outside of the area bounded by the Mach cone. The lift slope for the area within the Mach cone is given by:

$$\left(\frac{dC_L}{d\alpha}\right)_{x,y} = \frac{8}{\pi B}\sin^{-1}\sqrt{\frac{B(\frac{b}{2}-y)}{x}} \tag{27}$$

derived by Snow and Bonney.[1] This value differs from Equation (19) because the lift forces that give rise to the roll moment L_δ are a result of a uniform angle of attack at all points on the surface--namely the angle of cant.

Referring again to Figure 3,

$$K_{\ell_\delta} = (K_{\ell_\delta})_{\text{area I}} + (K_{\ell_\delta})_{\text{area II}} + (K_{\ell_\delta})_{\text{area III}} \tag{28}$$

For Area I:

From Equations (7), (22) and (27):

$$(K_{\ell_\delta})_I = \frac{\rho n_\delta \delta}{2} \int_{x=0}^{c} \int_{\mu=0}^{\tan^{-1}(\frac{1}{B})} \left(\frac{8}{\pi B} \sqrt{\frac{B(\frac{b}{2} - y)}{x}} \right) \frac{yx}{\cos^2 \mu} \, d\mu \, dx$$

and

$$(K_{\ell_\delta})_I = \frac{\rho n_\delta \delta}{B^2} \left(\frac{c^2 b}{4} - \frac{c^3}{4.8 B} \right) \tag{29}$$

For Area II:

From Equations (18) and (7)

$$(K_{\ell_\delta})_{II} = \frac{\rho n_\delta \delta}{2} \int_{x=0}^{B(\frac{b}{2} - y)} \int_{y=\frac{b}{2} - \frac{c}{B}}^{\frac{b}{2}} \frac{4}{B} \, y \, dx \, dy$$

and

$$(K_{\ell_\delta})_{II} = 2\rho n_\delta \delta \left(\frac{c^2 b}{4B^2} - \frac{c^3}{3B^3} \right) \tag{30}$$

For Area III:

From Equations (18) and (7)

$$(K_{\ell_\delta})_{III} = \frac{\rho n_\delta \delta}{2} \int_{a}^{\frac{b}{2} - \frac{c}{B}} \frac{4}{B} \, cy \, dy$$

and

$$(K_{\ell_\delta})_{III} = \frac{\rho n_\delta \delta}{B} \left(\frac{b^2 c}{4} - \frac{c^2 b}{B} + \frac{c^3}{B^2} - a^2 c \right) \tag{31}$$

---

[1] Snow, R. M., and Bonney, E. A., "Aerodynamic Characteristics of Wings at Supersonic Speeds", Bumblebee Report No. 55, The Johns Hopkins University Applied Physics Laboratory, March 1947.

And adding Equations (29), (30), and (31)

$$(K_{\ell_\delta}) = \frac{\rho n_\delta \delta}{B}\left(\frac{b^2 c}{4} + \frac{c^3}{8B^2} - a^2 c - \frac{c^2 b}{4B}\right) \tag{32}$$

3. Determination of the Conventional Aerodynamic Coefficients in Roll.

It is desirable to express any experimentally or theoretically determined coefficients in terms of the conventionally defined aerodynamic coefficients of roll, namely:

$C_{\ell_\delta} \equiv \frac{\partial C_\ell}{\partial \delta}$, roll moment derivative due to canted surfaces

$C_{\ell_p} \equiv \frac{\partial C_\ell}{\partial \left(\frac{pb}{2V}\right)}$, roll moment derivative due to rolling velocity

By definition:

$$L_\delta = C_{\ell_\delta} \; q \; A_p \; n_\delta \; \delta \; b = K_{\ell_\delta} \; V^2$$

and $$L_p = C_{\ell_p}\left(\frac{pb}{2V}\right) \; q \; A_p \; b \; n = K_{\ell_p} \; V \; p$$

Where $A_p \equiv$ area of tail or wing panel (defined as half of one exposed tail or wing surface, see Fig. 1)

Then

$$C_{\ell_\delta} = \frac{2K_{\ell_\delta}}{\rho \, b \, A_p \, n_\delta \, \delta} \tag{33}$$

$$C_{\ell_p} = \frac{4K_{\ell_p}}{\rho b^2 \, A_p \, n}$$

These coefficients may also be expressed in terms of the experimental constants C_1 and C_2 through use of equations (13a), (13b), and (33) as,

$$C_{\ell_\delta} = \frac{2 \, I \, C_2}{\rho \, b \, A_p \, n_\delta \, \delta} \tag{34}$$

$$C_{\ell_p} = \frac{4I}{\rho b^2 \, A_p \, n}\left(C_1 + \frac{K_R}{m}\right)$$

Comparisons of the experimental and theoretical values of C_{ℓ_p} and C_{ℓ_δ} offer a means of evaluating the accuracy of the linearized supersonic theory as applied here when used to calculate these quantities.

It will be noted from equation (32) that accurate measurements of the actual angle of incidence of each tail and wing panel is required for the theoretical determination of C_{ℓ_δ} for any missile tested.

METHOD OF DATA REDUCTION

The experimental values of the aerodynamic coefficients in roll for the missiles tested are determined by the following general procedure for reduction of the data obtained from the Aerodynamic Range.

A) Accurate measurements of the angular orientation in roll ($\emptyset$) and the linear position (z) of the missile in space are obtained from each of the photographic plates taken during the flight of the missile down the range. Very accurate measurements of the time at which 9 of the photographs were taken is determined from the chronograph record and megacycle counters.

B) The form of the solution $\emptyset = \emptyset(z)$ equation (15) of the theoretical roll equation is "fitted" to the measured values of $\emptyset$ and z, and the optimum values of the constants C_1 and C_2 in equation (15) are determined by the method of Differential Corrections.

C) The value of the retardation constant $\frac{K_R}{m}$ for the missile is determined by existing techniques using the measured values of z and the time t.

D) Values of the aerodynamic coefficients in roll are determined and their statistical accuracy (Probable Error) is computed.

The details of these four general steps will now be discussed.

A. Measurements from the Photographic Plates.

1. Angular Orientation in Roll. In order to determine the roll angle from the shadowgraphs of the missile (see Figure 4) it is first necessary to identify the quadrant in which a particular reference fin or wing occurs. Therefore one particular fin must be recognizable in both the vertical and horizontal photographs taken at each station. Identification of the fins was obtained, after considerable experimention, by locating a small pin in the trailing edge of each fin near the tip. The shape of the four pins differed as seen in Figure 4, and it was always possible to distinguish at least one of the shapes in both photographs and thereby definitely fix the quadrant of roll orientation. The roll angle of the missile at any station may be calculated from the coordinates of each of the identification pins (see Eq. 35) as obtained from the horizontal and vertical spark photographic plates using the usual methods of reduction of range data for obtaining the spatial position of a point from its images projected on the horizontal and vertical plates. (See Fig. 5).

$$\phi = \tan^{-1} \frac{\overline{AC} - \overline{CD}}{\overline{AD}}$$

$$\phi = \tan^{-1} \frac{\overline{BD} - \overline{AB}}{\overline{AD}} \qquad (35)$$

$$\phi = \tan^{-1} \frac{\overline{EG} - \overline{GH}}{\overline{EH}}$$

$$\phi = \tan^{-1} \frac{\overline{HF} - \overline{EF}}{\overline{EH}}$$

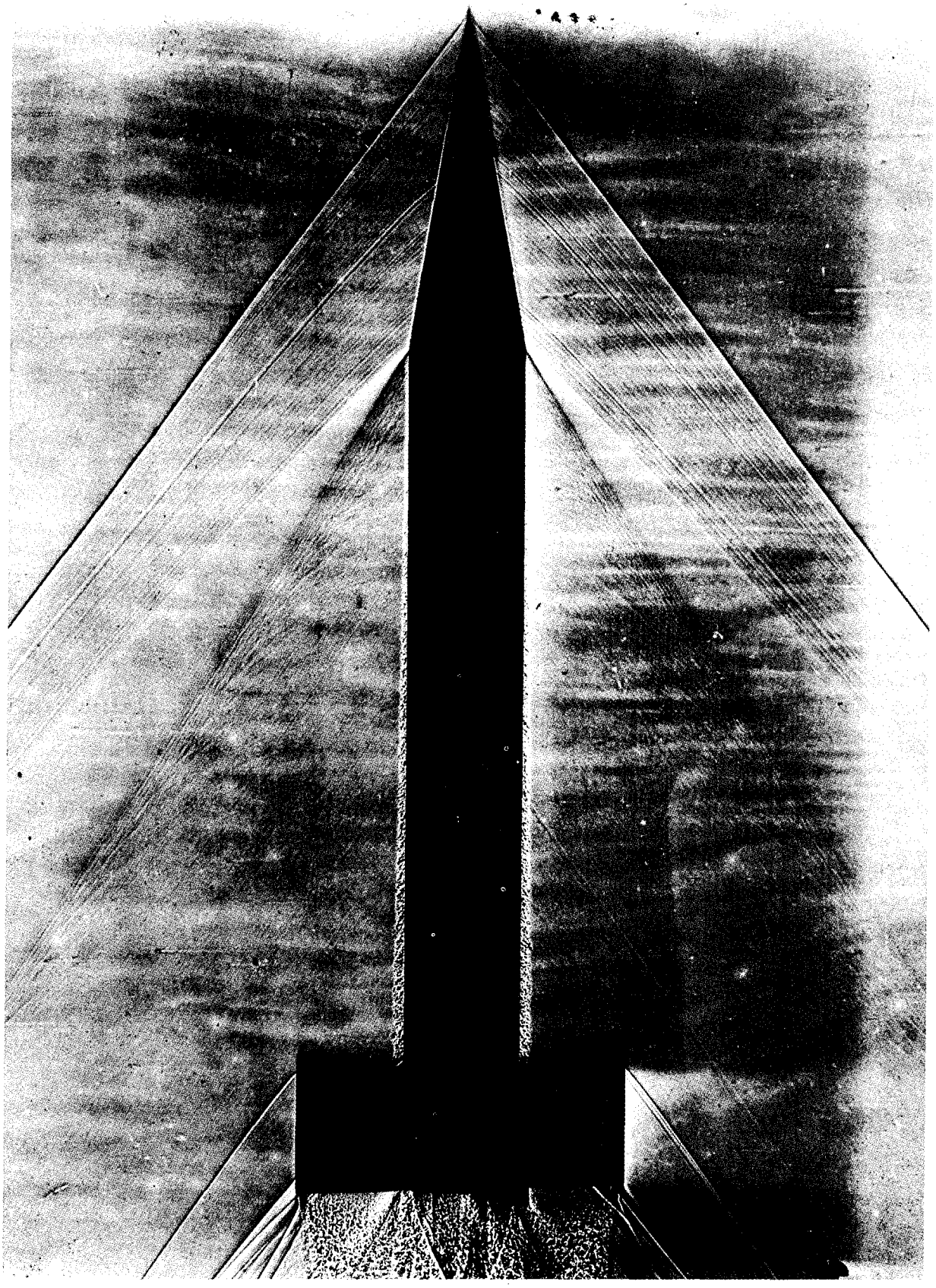

Figure 4. Shadowgraph of Roll Model in Free Flight.

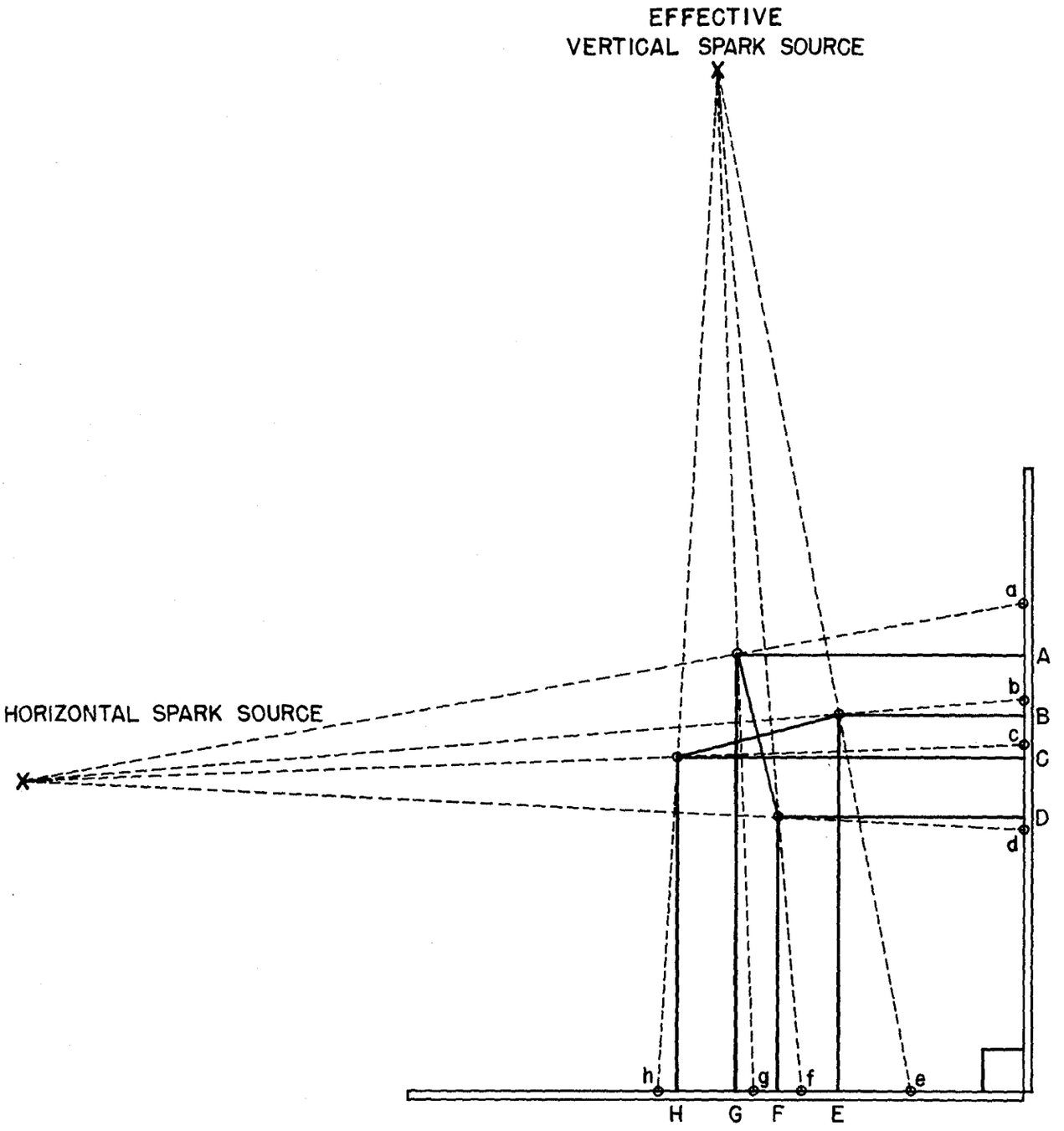
EFFECTIVE
VERTICAL SPARK SOURCE
HORIZONTAL SPARK SOURCE
a
b
c
d
A
B
C
D
h
g
f
e
H
G
F
E

FIGURE 5

The angular accuracy of the roll angle at a station is estimated to be $\pm$ .7° from a comparison of the four individual determinations made according to Eq. 35.

2. Linear Position of Missile. The location of a reference point on each station along the range is known to .001 feet. This reference point appears on the photographs and the location of the center of gravity of the missile in space at each station is accurately and simply determined by the technique presented by Charters and Thomas[1].

B. Determination of the Constants in the Roll Equation.

The constants C_1 and C_2 and at the same time the constants A, B, and s are determined by "fitting" the theoretical form of the roll equation (15), $\phi = \phi(z)$, to the ϕ, z data obtained from a particular firing. The process of "fitting" consists of first finding the initial or approximate values of the constants in equation (15) (designated as A_o, B_o, S_o, and C_{l_o}) and second applying the method of Differential Corrections to determine the optimum values of the constants.

1. Method of Differential Corrections.

Since the roll equation contains an exponential term, no method of least squares has been developed to handle this type of equation directly (at least not to the knowledge of the authors). However, the roll Equation (15) may be expanded by a Taylor Series about the initial values of the constants,

$$\phi = B_o + s_o z + A_o e^{-C_{l_o} z} + \Delta B + z\Delta s + e^{-C_{l_o} z}\Delta A - zA_o e^{-C_{l_o} z}\Delta C_1 -$$

$$ze^{-C_{l_o} z}\frac{\Delta C_1 \Delta A}{2} - ze^{-C_{l_o} z}\frac{\Delta C_1 \Delta A}{2} + z^2 A_o e^{-C_{l_o} z}\frac{(\Delta C_1)^2}{2} + \ldots$$

in which all terms in ΔC_1 and ΔA of order 2 or greater may be neglected if ΔC_1 and ΔA are small. Then

$$\phi_m - \phi_o = \Delta B + z\Delta s + e^{-C_{l_o} z}\Delta A - A_o z e^{-C_{l_o} z}\Delta C_1$$

where

$$\phi_o = (B_o + s_o z + A_o e^{-C_{l_o} z}) \; ; \text{ initial value of roll angle}$$

$$\phi_m = \text{measured value of roll angle}$$

is a linear relation and the differential corrections (ΔB, Δs, ΔA, and ΔC_1) to the initial value of the constants may be obtained by the usual least squares process. The corrected constants

$$A_1 = A_o + \Delta A \qquad s_1 = s_o + \Delta s$$

$$B_1 = B_o + \Delta B \qquad C_1 = C_{l_o} + \Delta C_1$$

may in turn be used as the initial values and the process repeated until the sum of the squares of the

[1] Charters, A. C. and Thomas, R. N., "The Aerodynamic Performance of Small Spheres from Subsonic to High Supersonic Velocities", JOURNAL OF THE AERONAUTICAL SCIENCES, Vol. 12, No. 4, P. 468, October 1945.

residuals[1] approaches a minimum. If the process is not convergent,[2] then either the roll equation does not represent the motion with sufficient exactness, or the initial values for the constants are not well determined.

Therefore, the successful application of the method of Differential Corrections depends upon a fairly accurate determination of the initial values of the constants. The techniques employed to obtain them are discussed in the following section.

2. Determination of the Initial Values for the Roll Constants.

(a) Steady State Rolling Velocity, (s_0). Differentiation of the roll equation (15),

$$\phi' = s - C_1 A e^{-C_1 z} \tag{36}$$

shows that as z increases, ϕ', the roll velocity, approached a constant value, s. The approximate value of ϕ'_∞ (designated s_0) may be determined from the range data in the following manner.

The average rolling velocity[3] ϕ' between successive, closely spaced stations is plotted for the value of z midway between the corresponding stations. The values of, ϕ'_1, ϕ'_2, ---- ϕ'_n taken from the resulting plot at equal but arbitrary intervals of distance (Δz) along the range are then substituted into equation (36)

$$\phi'_1 = s - C_1 A e^{-C_1 \Delta z}$$

$$\phi'_2 = s - C_1 A e^{-C_1 2\Delta z}$$

. . .

. . .

. . .

$$\phi'_{n-1} = s - C_1 A e^{-C_1 (n-1) \Delta z}$$

$$\phi'_n = s - C_1 A e^{-C_1 n \Delta z}$$

where the ratio of the differences between successive values of ϕ' becomes:

$$\frac{\Delta \phi'_n}{\Delta \phi'_{n-1}} = \frac{\phi'_n - \phi'_{n-1}}{\phi'_{n-1} - \phi'_{n-2}} = e^{-C_1 \Delta z} = \text{constant}$$

---

[1] Residual here is defined as the difference between the roll angle of the missile as measured and the angle calculated from the roll equation at any distance, z, along the range where the missile was photographed.

[2] If the sum of the squares of the residuals decreases with successive applications of the method of Differential Corrections, the process is convergent.

[3] This is determined simply by dividing the ϕ between adjacent stations by the corresponding distance between the stations.

or

$$\Delta \phi'_n = \Delta \phi'_{n-1} \; e^{-C_1 \Delta z} \tag{37}$$

From Equation (37) a table of $\Delta \phi'$ for any interval may be calculated since any difference $\Delta \phi'_n$ can be found from the previous known difference $\Delta \phi'_{n-1}$. Then the roll rate is given by [1]

$$\phi'_n = \phi'_1 + \Delta \phi'_2 + \Delta \phi'_3 + \ldots . \Delta \phi'_n$$

and the approximate steady state rolling velocity by:

$$s_o = \phi'_\infty = \phi'_1 + \sum_{n=2}^{\infty} \Delta \phi'_n$$

In practice, the interval of distance, Δz, used in reading from the curve of ϕ' versus Z was 50 feet, and that used in predicting $\Delta \phi'$ at distances greater than the length of the range was 100 feet. Values of $\Delta \phi'$ were predicted until they became of negligible magnitude.

(b) Damping Constant, (C_{1_o}). An initial value for the damping constant of the roll equation and a check on the value of s_o as previously determined, may be obtained from Equation (36) rewritten in terms of the approximate constants as:

$$\text{Log } \Omega = \log \left(C_{1_o} A_o \right) - C_{1_o} z = \text{Const} - C_{1_o} z \tag{38}$$

where

$$\Omega = s_o - \phi'$$

A plot of log Ω against Z, using the values of s_o and ϕ' previously calculated from the range data, should yield a straight line with slope, $\frac{d(\log \Omega)}{dz} = -C_{1_o}$ the damping constant. If the resultant plot is not quite a straight line, the value of s_o may be slightly changed until a constant slope for the plot is obtained.

(c) Boundary Constants, A_o and B_o. Although initial values for A and B may be obtained directly from equations (15) and (38) for z = 0, it was found to be a better procedure to solve for them from equation (15) alone by a least squares process using the range data and the approximated values for s_o and C_{1_o}.

3. "Fit" of the Roll Equation. The final equation representing the rolling motion of the missile is equation (15) written with the optimum values of the constants derived from the data by successive applications of the method of Differential Corrections until the sum of the squares of the residuals approaches a minimum. The fit of the final roll equation to the range data may then be evaluated by a comparison of the statistical magnitude of the final residuals with the magnitude of the estimated error in the

[1] This method was suggested by Dr. E. J. McShane, Professor of Mathematics, University of Virginia.

measurement of the roll angle from the photographic plates. The statistical magnitude of the final residuals is given by the usual statistical quantity, Probable Error[1];

$$P.E. = 0.6745\sqrt{\frac{\sum \Delta\bar{\phi}^2}{n-4}} \tag{39}$$

where

$\Delta\phi \equiv$ residual
$n \equiv$ number of observations

If the probable Error of the residuals is of the same order of magnitude as the estimated error in measurement of the roll angles from the shadowgraphs ($\pm$ .7°), then the final roll equation represents the best possible equation that can be written to fit the data and as such represents the true rolling motion of the missile within experimental accuracy.

C. Determination of the Value of the Retardation Constant, $\left(\frac{K_R}{m}\right)$.

The retardation constant defined by equation (9b) is proportional to the coefficient of drag of the missile. The constant then is determined in the conventional manner described in [2] where it is assumed that the time is given by a power series in the distance measured from the center of the range (z_o) as:

$$t = a_o + a_1(z - z_o) + a_2(z - z_o)^2 + \ldots\ldots$$

The coefficients a_o, a_1, a_2, etc., are determined from the experimental measurements by the method of Least Squares and the drag coefficient is in turn determined from these coefficients.

D. Aerodynamic Coefficients and the Statistical Precision

The values of the constants C_1 and C_2 of the roll equation, as determined by successive applications of the method of Differential Corrections, may be considered as the best values that the experimental data can yield. The roll coefficients C_{ℓ_p} and C_{ℓ_δ} are then determined simply by equation (34).

The effectiveness parameter, $\frac{p_s b}{2V}$, the steady-state tip Helix angle, may be obtained from the linearized theory by

$$\frac{p_s b}{2V} = \frac{sb}{2(57.3)}\left(\frac{K_{\ell_\delta}}{K_{\ell_\rho}}\right) \text{(radians)} \tag{40}$$

and from the experimental data by substitution of equations (13a) and (13b) into equation (40), whence;

$$\frac{p_s b}{2V} = \frac{b}{2(57.3)}\left(\frac{C_2}{C_1 + \frac{K_R}{m}}\right)$$

---

[1] Scarborough, J. B., "Numerical Mathematical Analysis", The Johns Hopkins Press, 1930.

[2] Charters, A. C. and Thomas, R. N., "The Aerodynamic Performance of Small Spheres from Subsonic to High Supersonic Velocities", JOURNAL OF THE AERONAUTICAL SCIENCES, Vol. 12, No. 4, P. 468, October 1945.

and using equation (16) gives:

$$\frac{p_s b}{2V} = \frac{sb}{2(57.3)} \left(\frac{1}{1 + \frac{K_R}{C_1 m}} \right) \tag{41}$$

The accuracy of the final aerodynamic coefficients is again expressed by the statistical quantity, Probable Error, (P.E.), dependent upon the P.E. of the coefficients in the roll equation. The general equations for the probable error of any function of independent quantities whose P.E.'s are known is given by:[1]

$$R = \sqrt{\left(\frac{\partial Q}{\partial q_1}\right)^2 r_1^2 + \left(\frac{\partial Q}{\partial q_2}\right)^2 r_2^2 + \cdots \left(\frac{\partial Q}{\partial q_n}\right)^2 r_n^2} \tag{42}$$

where

$$Q = f(q_1, q_2, q_3, - - - q_n)$$

and R, r_1, r_2, - - - r_n are the P.E.'s of Q, q_1, q_2, - - q_n respectively, determined by Equation (39).

EXPERIMENTAL TESTS

The purpose of the experimental program is not to present a finished research program but rather to investigate the suitability of the Aerodynamic Range to the free-flight roll technique presented in this paper. Specifically, the purpose may be restated in three parts:

1) To determine the accuracy of agreement of the theoretical roll equation with the experimental data measured in the Aerodynamic Range as well as to determine the accuracy of the reduction methods used to obtain the roll constants (aerodynamic coefficients) from the data.

2) To determine the ability of the combined Range and technique to accurately reproduce aerodynamic coefficients.

3) To compare the experimental and theoretical values of the aerodynamic coefficients.

A. Experimental Apparatus and Procedure

1. Aerodynamic Range

The Aerodynamic Range and the test procedure are described briefly in the introduction to this paper. Further details are presented by Charters and Thomas[2] and Figure 6. A unique modification to the equipment is the special "railed" gun (shown in Figure 7) used for launching winged and/or finned missiles. In the operation of the gun, the projectile is guided by its body in the central cylindrical portion of the barrel, the fins or wings riding freely in the slots.

2. Design of Missiles for Firing Program

To fulfill the purposes of the program, a single missile design was chosen consisting of the simplest configuration from a construction standpoint as well as from a standpoint of amenability to

[1] Scarborough, J. B., "Numerical Mathematical Analysis", The Johns Hopkins Press, 1930

[2] Charters, A. C. and Thomas, R. N., "The Aerodynamic Performance of Small Spheres from Subsonic to High Supersonic Velocities", JOURNAL OF THE AERONAUTICAL SCIENCES, Vol. 12, No. 4, P. 468, October 1945.

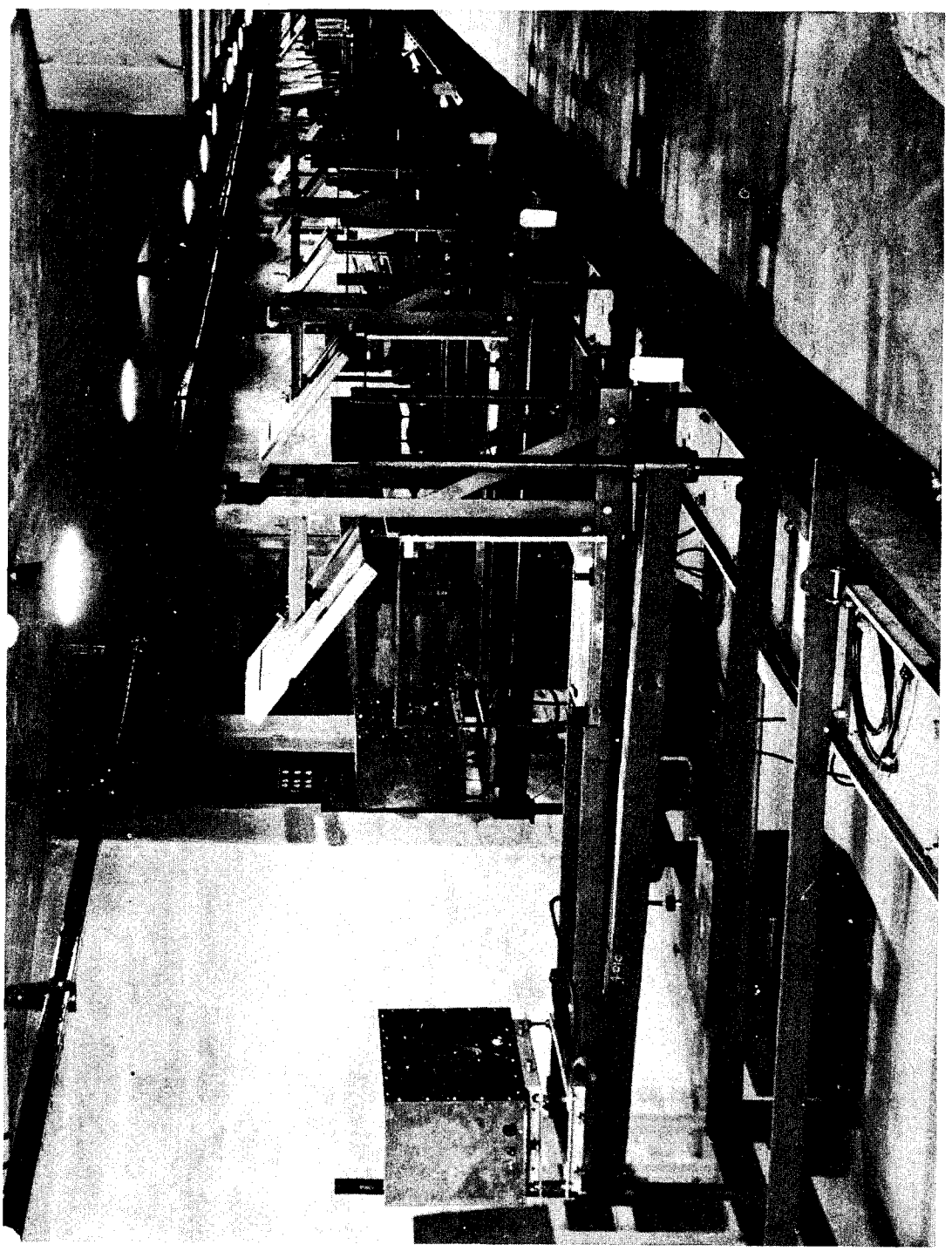

Figure 6. Aerodynamic Range.

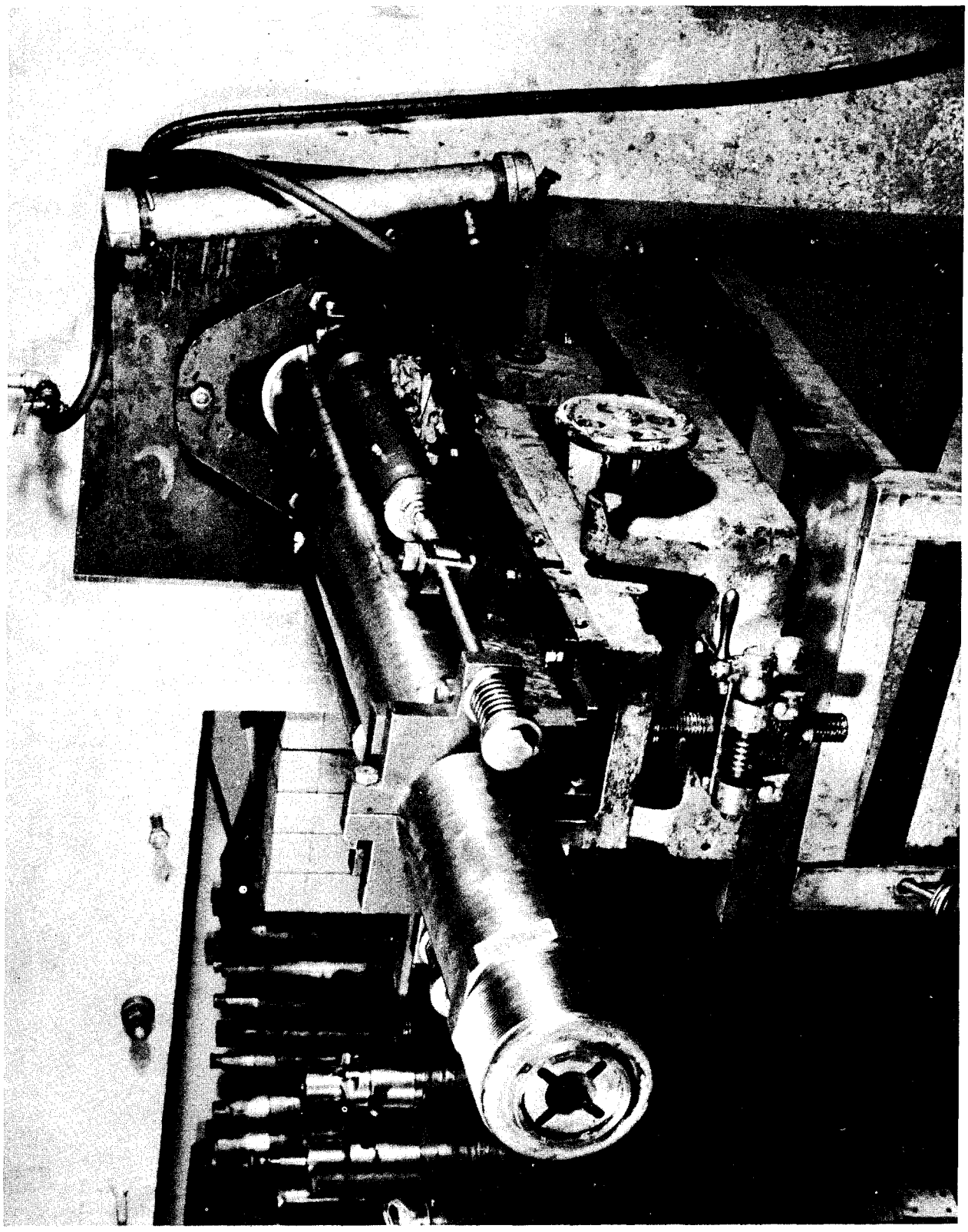

Figure 7. Special Railed Gun.

theoretical supersonic aerodynamic calculations. The missile design is shown in Figure 8, and consists of a cone-cylinder fuselage with four rectangular fins in cruciform arrangement. The fin surfaces are wedge shaped with 16% maximum thickness and were constructed as shown in the fin detail of Figure 8, for reasons of simplicity. On each model, two of the tail fins were canted.

For two of the models, the fuselage was of aluminum with wings of Tobin bronze. Bronze wings were used to obtain (1) a higher moment of inertia in roll in order to decrease the rate of acceleration in roll and correspondingly lengthen the curved portion of the measured roll displacement - distance curve, and (2) a higher mass in order to decrease the linear deceleration of the missile and result in more nearly constant-velocity flight. The remaining two models were machined entirely from Tobin bronze to further increase the moment of inertia in roll. A summary of the missile design is given below.

TABLE I

Missile No.	Average Angle of Cant on two Tail fins,	Material	Moment of Inertia in roll - I_2 (slugs-ft^2)	Mass of Missile - m (slugs)
1	2.029°	Aluminum fuselage + Bronze fins	1.240×10^{-5}	1.224×10^{-2}
2	4.288°	Aluminum fuselage + Bronze fins	1.235	1.221
3	2.108°	All bronze	2.186	3.068
4	4.454°	All bronze	2.210	3.067

B. Results and Discussion

The four missile models (Table I) were gun launched at an intended Mach number of about 1.7. The actual Mach number that resulted in the four flights both at the beginning and end of the trajectory as well as the air density and velocity of sound in the range are recorded in Table II.

TABLE II

Missile No.	Mach No. at beginning of trajectory	Mach No. at end of trajectory	Mach No. at center of timing data	Vel. of Sound in Range (Ft/Sec)	Air Density in Range (Slugs/Ft^3)
1	1.790	1.675	1.746	1135	2.297×10^{-3}
2	1.752	1.635	1.694	1131	2.296
3	1.621	1.575	1.592	1121	2.357
4	1.665	1.616	1.637	1120	2.357

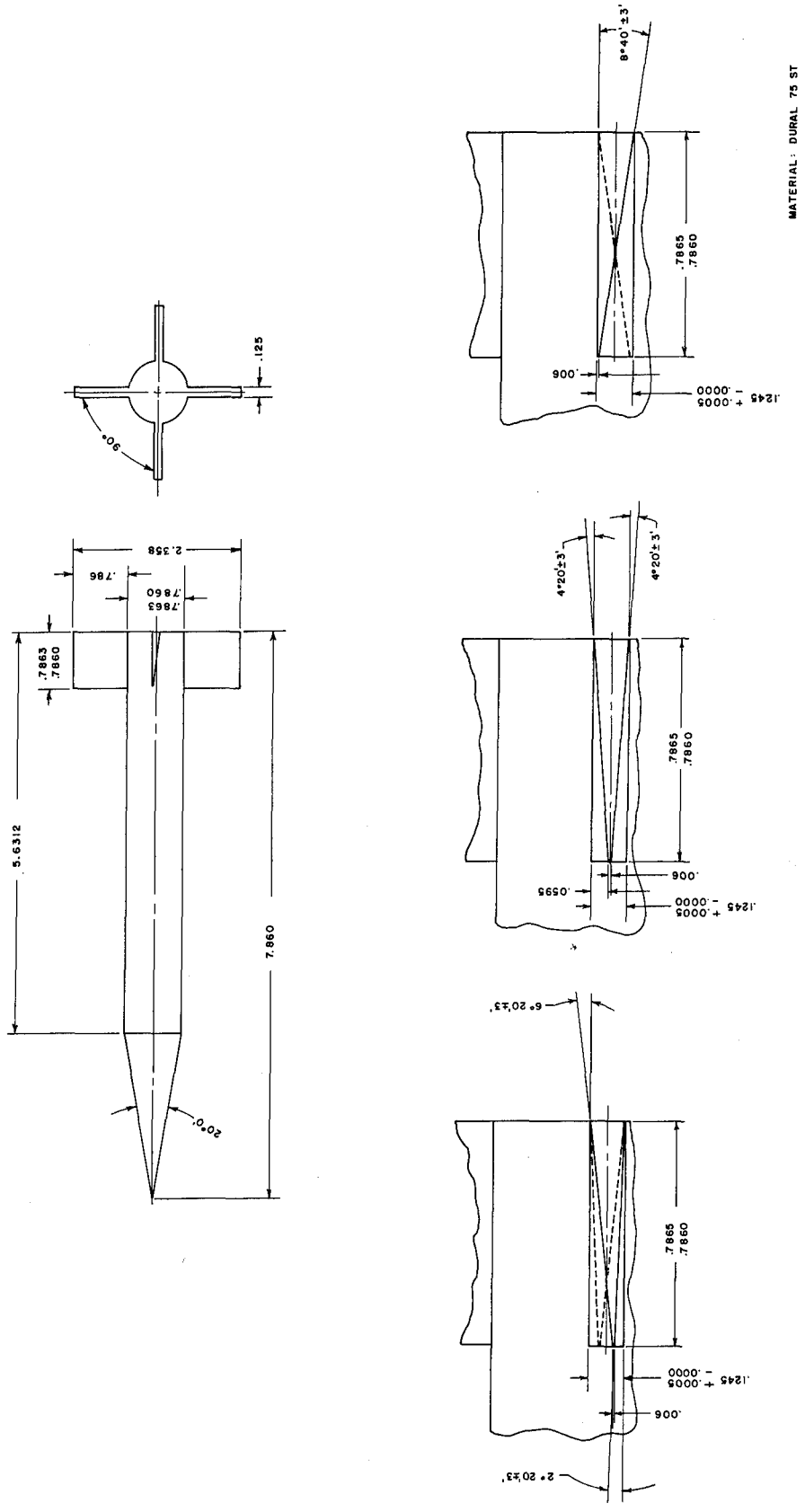

FIGURE 8 – DESIGN OF MISSILES USED IN THE EXPERIMENTAL TESTS

1. Rolling Motion

The angular orientation in roll of the models as measured from the shadowgraphs taken at each spark station along the trajectory is shown by the points in Figure 9. In this same figure are plotted the equations of the curves which best fit the data as obtained by the methods discussed in the previous section.

The difference between the curves for missiles number 2 and 1 as well as number 4 and 3 are a result of the differences in the angles of cant employed. The differences between the curves for missiles number 2 and 4 as well as number 1 and 3 are due primarily to the differences in the roll moment of inertia (see Table I).

The use of a greater moment of inertia, it was felt, would result in a better determination of the roll coefficients because of the slower roll acceleration rate and linear deceleration rate. However, no such variation in experimental accuracy with moment of inertia can be noted in the results and the accuracy appears dependent only upon the exactness of the measurements obtained from the spark photographs.

The excellent "fit" of the roll equation to the experimental points which cannot be observed in Figure 9 because of size limitations is given in Table III as the statistical quantity, Probable Error:

TABLE III

Model	1	2	3	4
P. E.	.26°	.73°	.65°	.57°

Since the Probable Error is small and of the same order of magnitude as the estimated error in roll angle measurement, it may be concluded that the roll equation represents the actual motion of the models tested to within the experimental error. It therefore appears that the rolling motion is unaffected by the pitching motion for the mean square yaws encountered in the tests (see Table IV).

The optimum values of the constants in the roll equation were obtained by the methods outlined in the Data Reduction Section and are given with their Probable Error in Table IV as determined from the reduction.

TABLE IV

Model	1	2	3	4
A	660°	1386	882	2285
B	-621°	-1298	-838	-2079
C_1	.0166	.0169	.0096	.0098
P.E.	.24%	.34	2.34	.53
s	14.90	32.02	15.57	32.64
P.E.	.04%	.05	.57	.15
$C_2 = C_1 s$	.2466	.5418	.1502	.3211
P.E.	.24%	.34	2.41	.55
$\left(\frac{K_R}{m}\right)$	2.7×10^{-4}	2.8	1.2	1.2
P.E.	.7%	.1	1.1	.4
$\overline{Yaw}^2$	1.48°	.34	.35	1.15
No. of obser.	14	21	16	18

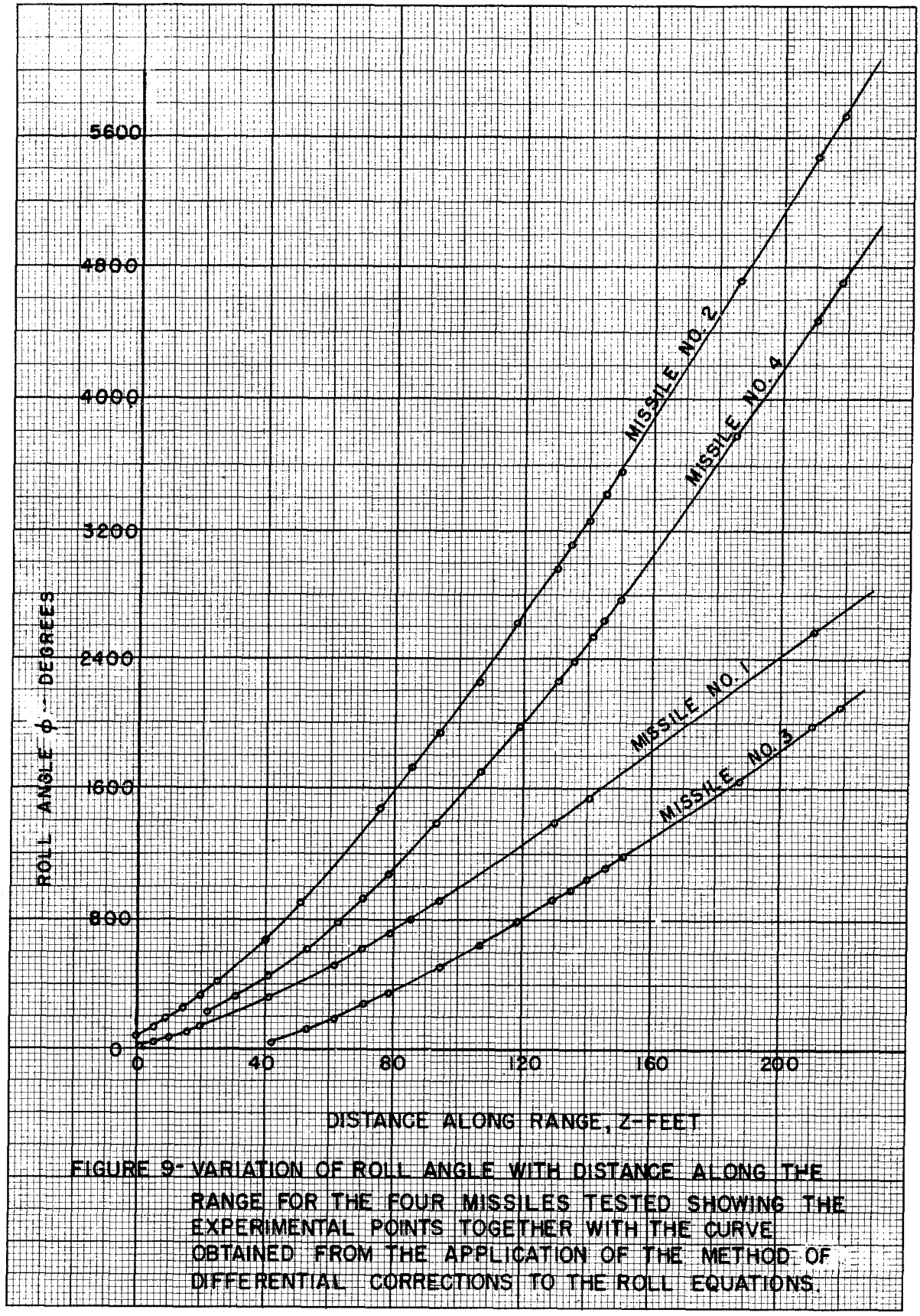

FIGURE 9- VARIATION OF ROLL ANGLE WITH DISTANCE ALONG THE RANGE FOR THE FOUR MISSILES TESTED SHOWING THE EXPERIMENTAL POINTS TOGETHER WITH THE CURVE OBTAINED FROM THE APPLICATION OF THE METHOD OF DIFFERENTIAL CORRECTIONS TO THE ROLL EQUATIONS.

2. Aerodynamic Coefficients

The experimental values of aerodynamic coefficients for the models tested may be obtained from the data in Table IV and Equation 34. The theoretical values of the coefficients for the models are obtained from Equations 26, 32 and 33. The values for the coefficients are given in Table V and their very good quality is again indicated by the statistical factor, Probable Error, the significance of which is discussed in the Method of Reduction Section.

The experimental values of C_{ℓ_p} and C_{ℓ_δ} (given in Table V) and the theoretical curves are plotted respectively in Figures 10 and 11 against the average flight Mach number. (See Table II). It is seen from the figures that the values for model 3 do not fall in line with those for the other models. It may be seen from Table V that the P.E.'s for model 3 are more than four times as large as the largest P.E. for the other three models. This is a positive indication that the reduction of model 3 is weak, in comparison. It is further noted in Figure 9, that model 3 is lacking stations at the beginning of the range where data are required for a good determination of C_1. The dashed line in the figures represents the theoretical slope at an average Mach number drawn thru the weighted average of the coefficients at this average Mach number (See "Internal Consistency and Reproducibility of the Data, and Linearity" Sect. 4 following).

The weighted average experimental value of C_{ℓ_p} at the reduced Mach number as indicated by the dashed curve in Figure 10 is 21.0% greater than the value calculated from the linearized theory as applied in this paper (no body-wing interference) and the corresponding value of C_{ℓ_δ} in Figure 10 is only 7.6% greater than the theoretical. (See Table VI)

Concerning this deviation of the experimental values from the theoretical it will be remembered that the airfoil section used was of triangular shape (single wedge), with about 16% maximum thickness at the trailing edge. A comparison of the theoretical lift of an infinite-aspect-ratio wing of such cross section obtained by the linearized theory with that obtained from the exact theory using the oblique shock equations results in approximately a 15% lower value for the linearized lift at a Mach number in the neighborhood of 1.7.

In view of the above results one is tempted to speculate. The difference between the experimental and the theoretical values for C_{ℓ_p} might immediately be attributed to the fact that the fins were of such large thickness that the linearized theory simply failed to predict the correct magnitude of pressures acting upon them. However, from Figure 10, the fact that the experimental values of C_{ℓ_δ} deviate only 7.6% from the calculated values (instead of about 21.0% as was the case for C_{ℓ_p}) must obviously modify this first observation in the following manner. Let us assume that at any point on the fin the actual values of the lift slope $\left(\frac{dC_L}{d\alpha}\right)$ for the two roll moments are equal except for a small deviation in the tip region (see Figure 12b) as is indicated by the theory when the rectangular fins are considered attached to an infinite wall, and let us consider the theoretical $\left(\frac{dC_L}{d\alpha}\right)$ distributions shown by the solid lines in Fig. 12b. Then, if the above assumption is reasonably correct, since C_{ℓ_p} depends upon the value of y^2 in the integration (see Figure 1) and C_{ℓ_δ} upon y, the respective deviations of the experimental results of C_{ℓ_p} and C_{ℓ_δ} from the calculated

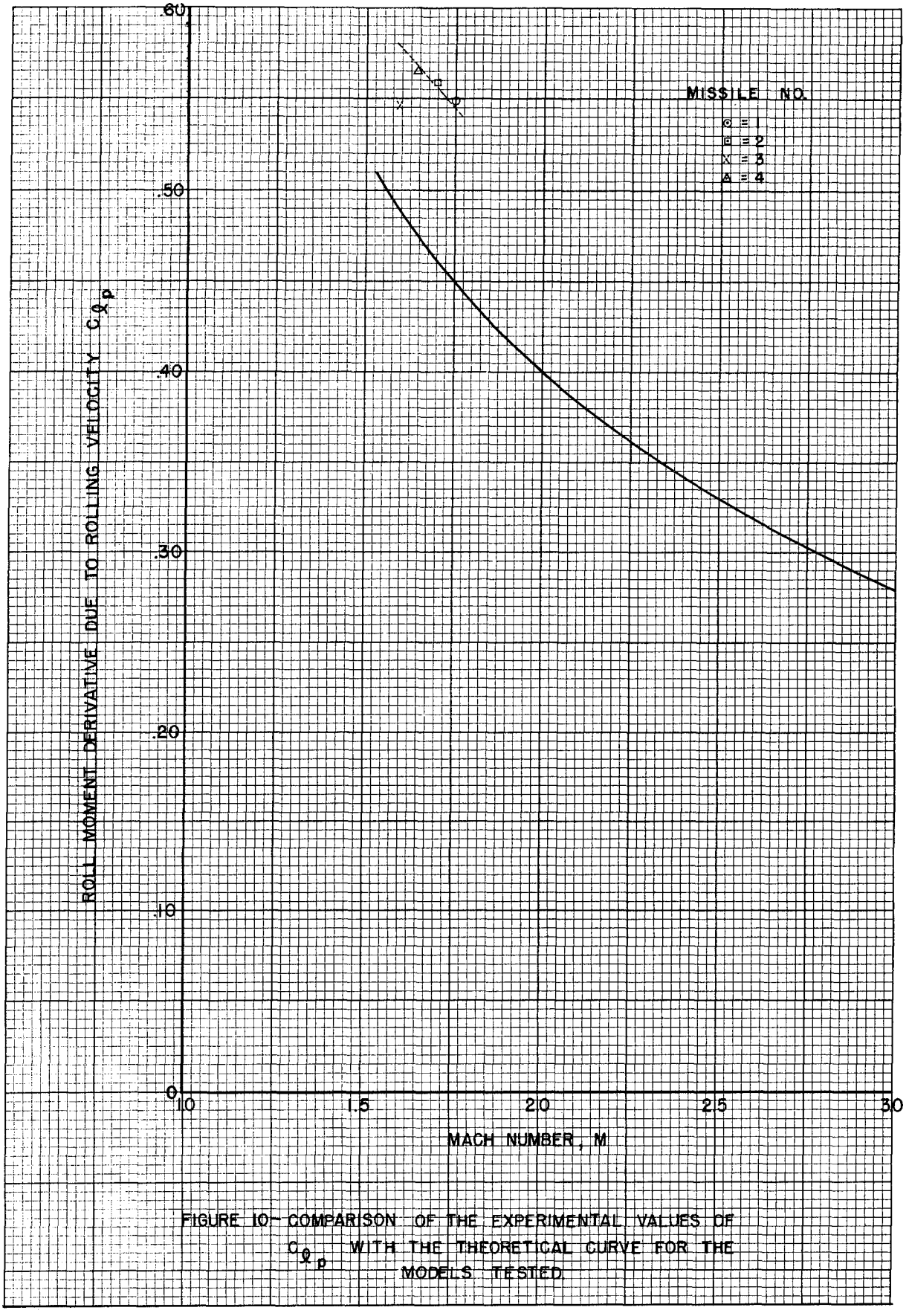

FIGURE 10- COMPARISON OF THE EXPERIMENTAL VALUES OF C_{ℓ_p} WITH THE THEORETICAL CURVE FOR THE MODELS TESTED.

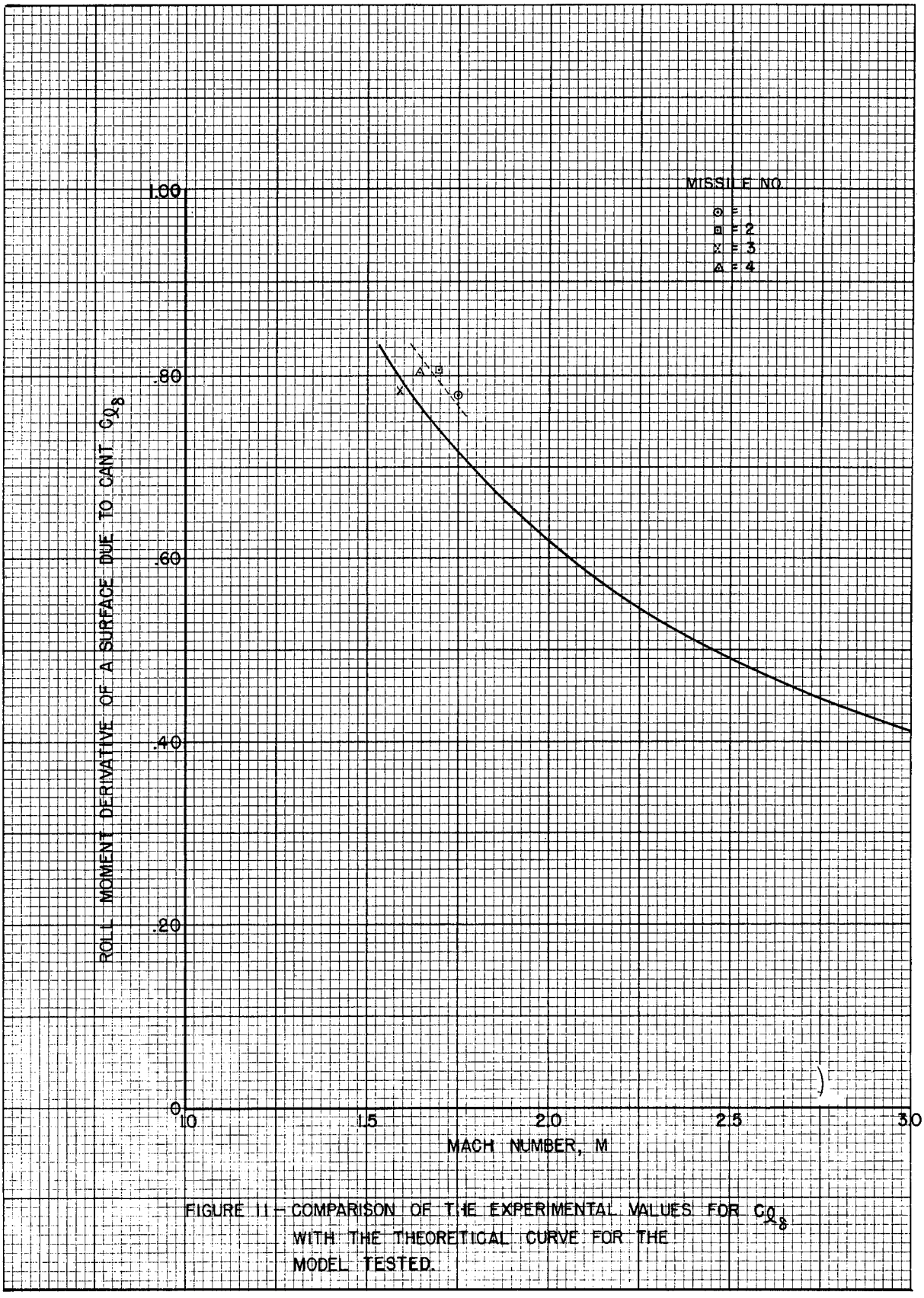

FIGURE 11 – COMPARISON OF THE EXPERIMENTAL VALUES FOR C_{l_δ} WITH THE THEORETICAL CURVE FOR THE MODEL TESTED.

values indicate that, in addition to the magnitude, the actual distribution of pressure on the fin surface differs appreciably from the assumed theoretical distribution; and it may be inferred that this distribution of pressure must be somewhat distorted from the calculated pattern in a manner qualitatively shown in Figure 12a with greater pressures acting over the area in the region near the wing tips. Such a pressure distribution would result in a somewhat lopsided lift-slope distribution over the fin as indicated in Figure 12b and may be a combined result of the large fin thickness employed, (particularly critical at the fin tip) and the wing-body interference.

3. Effectiveness Parameter

The experimental values for the effectiveness parameter (obtained from equation (40), Table IV, and the physical measurements) and the theoretical values for this parameter (obtained from the equations (26), (32), and (41)) are given in Table V together with their Probable Error as obtained from the reduction. Figure 13 gives the theoretical curve for the effectiveness parameter per δ vs Mach number together with the experimental points. It is noted that the experimental points are approximately 11.3% lower than the theory. See Table VI. This difference is due to the ratio of C_{ℓ_δ} to C_{ℓ_p} (see Eq. 41); these coefficients were discussed in paragraph 2. (Aerodynamic Coefficients).

TABLE V

Model	1	2	3	4
Mach No.	1.746	1.693	1.592	1.637
C_{l_p} (th.)	.449	.460	.483	.472
C_{l_p} (ex.)	.548	.559	.546	.564
P. E.*	.24%	.33	2.32	.52
C_{l_δ} (th.)	.716	.740	.794	.769
C_{l_δ} (ex.)	.778	.806	.784	.802
P. E. *	.24%	.34	2.41	.55
$\frac{p_s b}{2V}$ (th.)	.0283	.0602	.0303	.0633
$\frac{p_s b}{2V}$ (ex.)	.0247	.0531	.0260	.0546
P. E. *	.04%	.05	.59	.15

*The low values for the Probable Errors indicate that the coefficients are rather well determined from the reductions.

4. Internal consistency or Reproducibility of the Data, and Linearity

The internal consistancy or reproducibility of the data was estimated by reducing the experimental values of C_{ℓ_p}, C_{ℓ_δ}, and $\frac{p_s b}{2V} \Big/ \delta$ to a common Mach number of M = 1.665 by the theoretical value

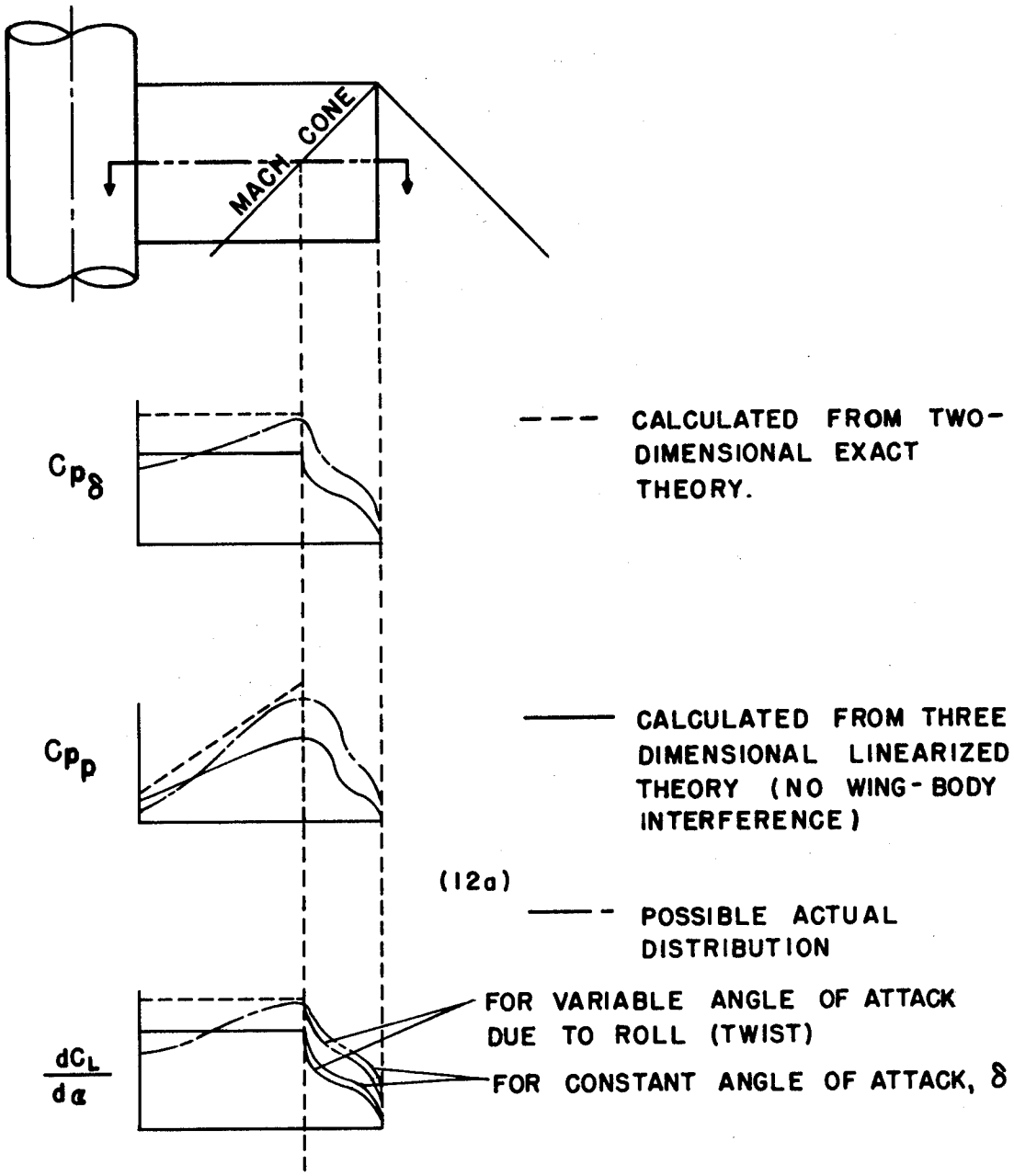

FIG. 12 – DISTRIBUTION ON THE FIN PANEL OF (a) THE COEFFICIENTS OF PRESSURE DUE TO CANT AND ROLLING VELOCITY AND (b) OF THE LIFT SLOPE.

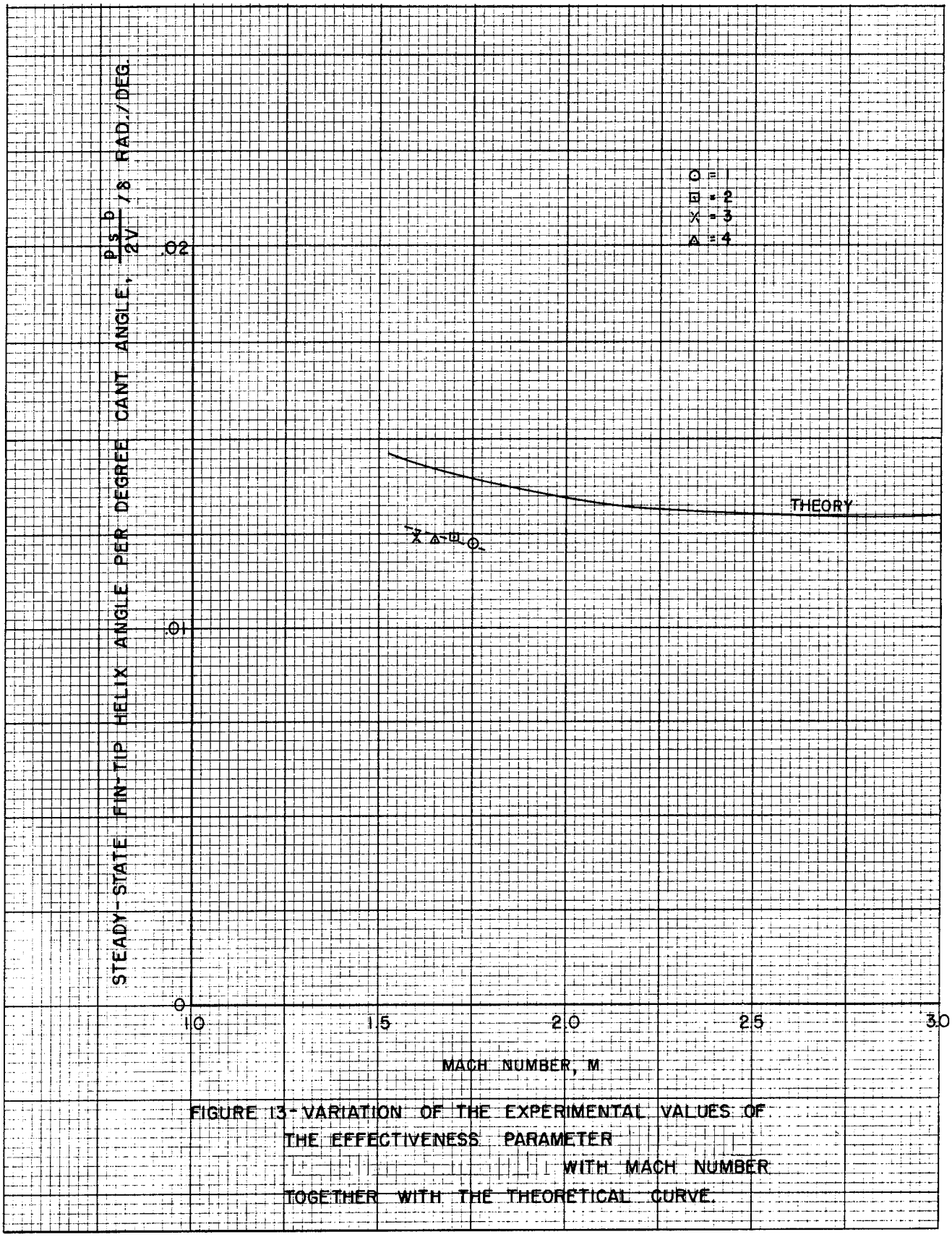

FIGURE 13- VARIATION OF THE EXPERIMENTAL VALUES OF THE EFFECTIVENESS PARAMETER WITH MACH NUMBER TOGETHER WITH THE THEORETICAL CURVE.

of the slopes at M = 1.665. These reduced values are given in Table VI.

The weighted average was obtained from [1]

$$\frac{\sum\left(\frac{c}{P.E.^2}\right)}{\sum\left(\frac{1}{P.E.^2}\right)} = \text{Weighted Average}$$

and the Probable Error of the weighted average from [1]

$$0.6745\sqrt{\frac{W_1 V_1^2 + W_2 V_2^2 + W_3 V_3^2 + W_4 V_4^2}{(n-1)(W_1 + W_2 + W_3 + W_4)}}$$

where

$$W = \frac{1}{P.E.^2} \qquad n = 4$$

V = Diff. of coeff. at same Mach No. from average.

These values of Probable Error are a measure of the internal consistancy or reproducibility of the data and their small values indicate that the technique is quite promising.

The theoretical values of the coefficients at the common Mach number are also given in Table VI together with their deviation from the experimental weighted average.

In plotting C_{ℓ_δ} vs M it was assumed that C_ℓ was linear with δ ; this assumption may now be investigated by plotting C_ℓ vs δ where

$$C_\ell = C_{\ell_\delta}\,\delta$$

It is seen in Figure 14 that the assumption of linearity is consistant with the experimental results.

TABLE VI

Model	Mach No	C_{ℓ_p}	C_{ℓ_δ}	$\frac{p_s b}{2V}\Big/\delta$
1	1.665	.566	.820	.01241
2	1.665	.565	.821	.01247
3	1.665	.530	.746	.01215
4	1.665	.557	.787	.01218
Weighted Average		.564	.816	.01242
P.E. of Wt. Av.		.27%	.55%	.26%
Theory		.466	.758	.014
Deviation of Weighted Average from Theory		21.0%	7.6%	-11.3%

In Figure 15 the effectiveness parameter is plotted vs δ and it is seen to be linear, in good agreement with theory.

[1] Scarborough, J. B., "Numerical Mathematical Analysis", The Johns Hopkins Press, 1930

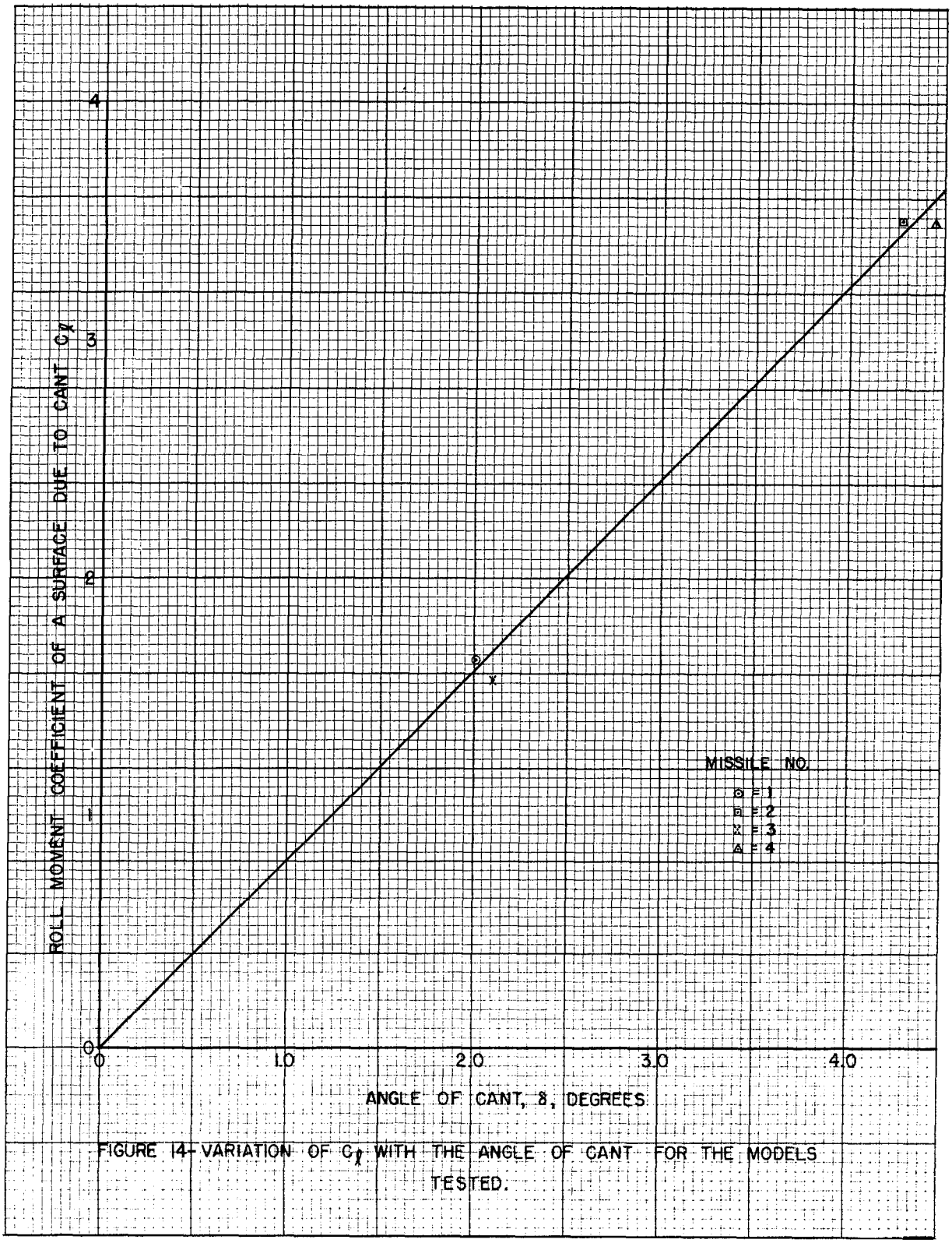

FIGURE 14- VARIATION OF C_{ℓ} WITH THE ANGLE OF CANT FOR THE MODELS TESTED.

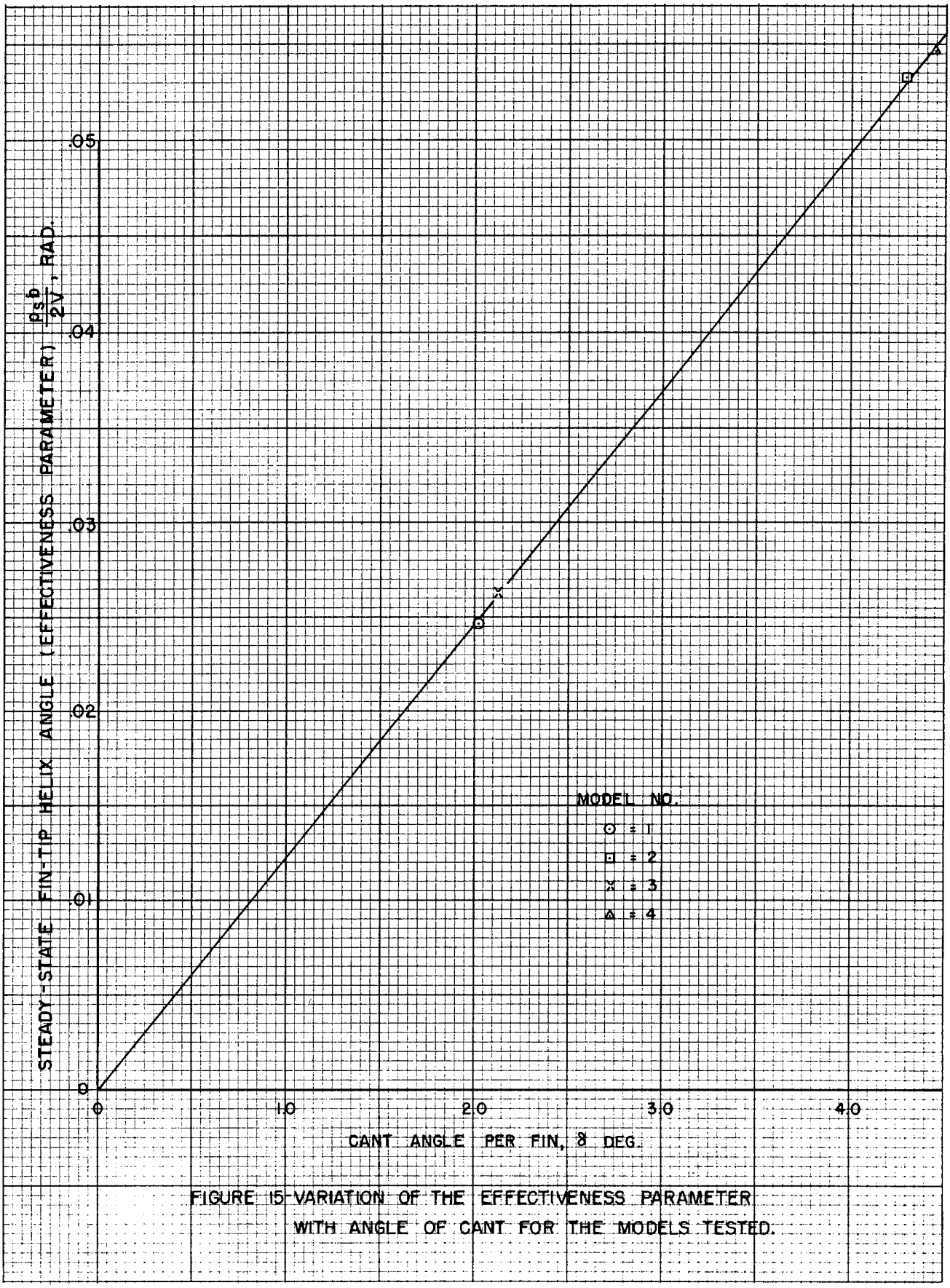

FIGURE 15 VARIATION OF THE EFFECTIVENESS PARAMETER WITH ANGLE OF CANT FOR THE MODELS TESTED.

CONCLUSIONS

1. The tests establish the validity of the roll equation for accurately representing the true motion of the missile as well as the accuracy of the reduction methods employed since the probable error of the residuals of the "fitted" equation is a maximum of .73° and is of the same magnitude as the estimated error in the roll angle measurements.

2. The tests show that the rolling moment coefficient due to cant and the effectiveness parameter depend linearly on the angle of cant for angles of cant less than 4.5°.

3. The tests show that the experimental values of the coefficients, C_{ℓ_p} and C_{ℓ_δ}, as obtained from a 16% thick wing are respectively 21.0% and 7.6% larger than the values calculated from the three-dimensional linearized theory, and that the experimental value of $\frac{p_s b}{2V}\Big/\delta$ is 11.3% less than theory.

4. The tests establish the excellent reproducibility of the aerodynamic coefficients as shown by the weighted Probable Errors of .27% for C_{ℓ_p}, .55% for C_{ℓ_δ}, and .26% for $\frac{p_s b}{2V}\Big/\delta$ when the values of the coefficients are reduced to a common Mach number.

ACKNOWLEDGEMENTS

The authors acknowledge the assistance of Dr. A. C. Charters in the analysis and presentation of the results, and of Miss Karolyn Skegas in developing new methods of reducing the experimental data.

Ray E. Bolz

John D. Nicolaides

APPENDIX A

A. Rolling Moments Due to Angle of Attack α and Angle of Yaw β

These two moments are identical in nature because of the symmetry of the missile surfaces. The magnitude of such a moment is given by:

$$L = \frac{\partial C_L}{\partial \beta} \quad \beta \quad \frac{\rho V^2}{2} \quad S_{w,t} \quad b$$

where $S_{w,t}$ is the area of the wing, tail, or both. Then

$$L = \left[\frac{\alpha}{B^2} \left(\frac{1 - B^2}{AB} - \frac{3 + B^2}{3A^2B^2} \right) \right] \quad \frac{v}{V} \quad \frac{\rho V^2}{2} \quad S_{w,t} \qquad \text{(I)}$$

where the expression for $\frac{\partial C_L}{\partial \beta}$ has been obtained from Reference 4 and β now is replaced by the ratio v/V, where v is the sideslip velocity. In equation (I), "A" is defined as the aspect ratio of the surface considered. Now when α, the angle of attack, is replaced by its equivalent w/V, where w is the component of missile velocity in the vertical plane; equation I becomes:

$$L = \left[\frac{1}{B^2} \left(\frac{1 - B^2}{AB} - \frac{3 + B^2}{3A^2B^2} \right) \right] \quad \frac{\rho S_{w,t} b}{2} \quad (vw) \qquad \text{(II)}$$

But (vw) is the product of two very small disturbance velocities compared with V and as such the moment is of second order and negligible for a rolling missile.

B. Rolling Moments Due to Pitching and Yawing Angular Velocities

Inspection immediately shows that these coefficients also depend upon the product of two very small quantities (qv) and (rw) respectively. Therefore such rolling moments are negligible and need no further consideration.

APPENDIX B

REDUCTION OF ROLLING MOTION OF MISSILE 4

1. DATA

The shadowgraphic plates obtained from the operative stations in this firing were placed on an illuminated grid consisting of 20 divisions per inch where measurements were made of (1) the locations of the identification pins (See Figure 5, a, b, c, d, ...etc.) and (2) the linear position of the missile with respect to the datum point in the photograph. From the measurements of the pins, the coordinates of the pins may be determined from the geometry at the station and thus the roll orientation may be calculated from Equation 35. These data of roll angle and linear position are given in Table VII and are plotted in Figure 9.

TABLE VII

Sta.	Z (ft)	$\phi°$	$\Delta\phi°$	Z (ft)	ϕ' o/ft.	$\bar{Z}$ ft.
5	0	205.76				
			107.41	9.6238	11.16	4.8119
6	9.6238	313.17				
			146.99	11.0271	13.33	15.1374
7	20.6509	460.16				
			167.04	11.0347	15.14	26.1682
8	31.6856	627.20				
			169.34	9.9845	16.96	36.6778
9	41.6701	796.54				
			144.75	7.8427	18.46	45.5914
10	49.5128	941.29				
			157.40	8.1573	19.30	53.5914
11	57.6701	1098.69				
			329.47	15.8524	20.78	65.5963
13	73.5225	1428.16				
			271.14	12.0822	22.44	79.5636
14	85.6047	1699.30				
			281.53	11.9903	23.48	91.5999
15	97.5950	1980.83				
			295.97	12.0661	24.53	103.6280
16	109.6611	2276.80				
			125.34	5.0372	24.88	112.1797
17	114.6983	2402.14				
			127.84	4.9560	25.79	117.1763
18	119.6543	2529.98				
			128.02	4.8814	26.23	122.0905
19	124.5357	2658.00				
			130.25	5.0552	25.76	127.0633
20	129.5909	2788.25				
			985.49	36.0178	27.36	147.5998
21	165.6087	3773.74				
			687.80	23.9589	28.71	177.5882
24	189.5676	4461.54				
			240.10	8.1727	29.38	193.6540
25	197.7403	4701.64				

2. Initial values for the constants.

From the differences in the roll angles and the linear distances between successive stations approximate values of ϕ' (deg/ft) at a point midway between the station may be obtained. These values of ϕ' and Z are also given in Table VII and are plotted in Figure 16.

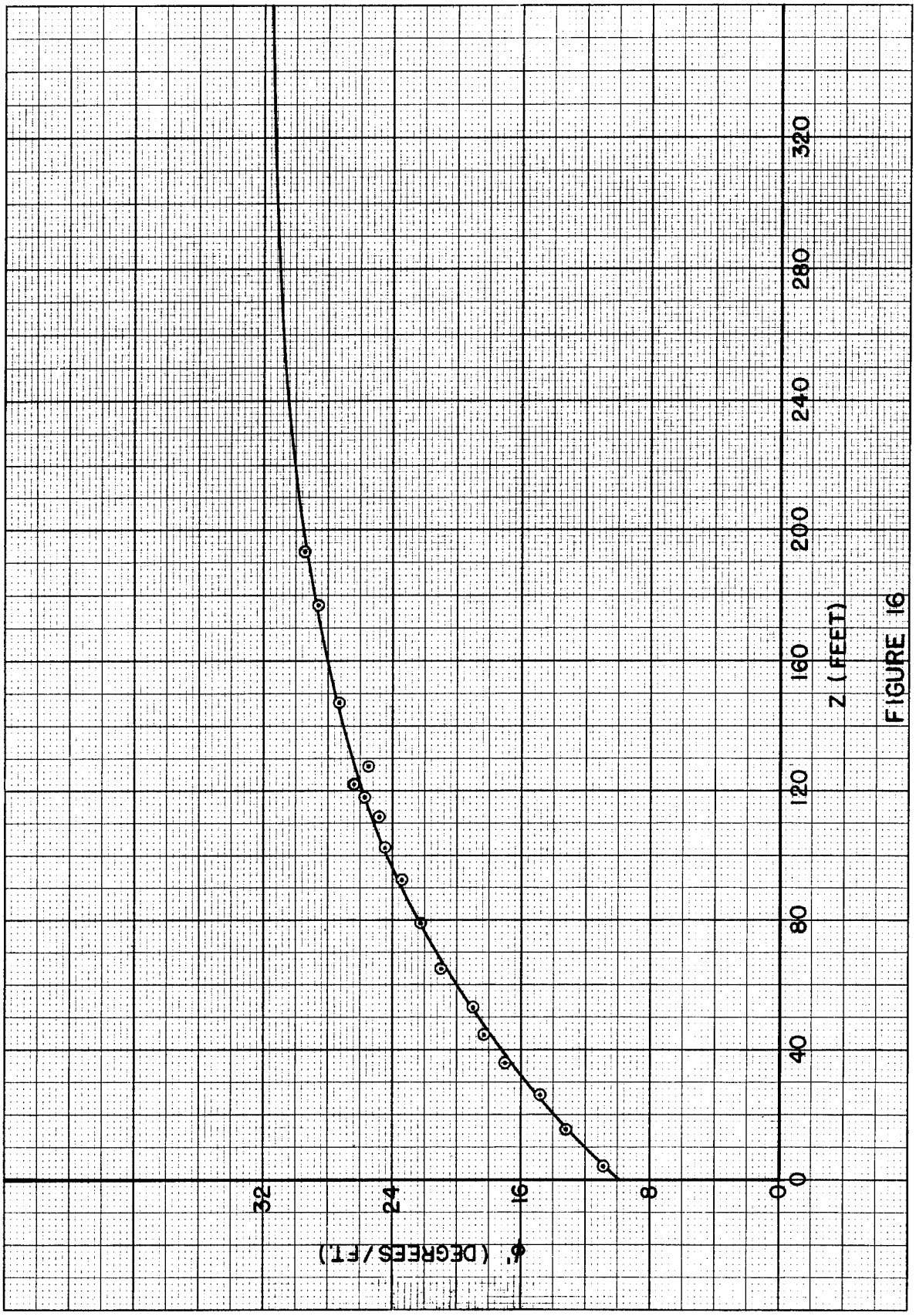

FIGURE 16

From the data given in Table VII, an initial value of s may be obtained by the method indicated in the section on "Method of Data Reduction" 2, (a) as illustrated in Table VIII.

TABLE VIII

Z	ϕ'	$\Delta \phi'$	Ratio
0	10.00	10.00	
		14.40	
100	24.40		2.769
		5.20	
200	29.60		
		1.859	
300			
		.671	
400			
		.242	
500			
		.087	
600			
		.031	
700			
		.011	
800			
		.004	
900			

$$\sum = 32.505 = s_o$$

An initial value of C_1 may be obtained from the slope of the logarithmic plot of $(s_o - \phi')$ vs Z (see section on "Method of Data Reduction" 2, (b), Table IX and Figure 17.

TABLE IX

Z	ϕ'	$s_o - \phi'$
0	10.00	22.505
50	18.60	13.905
100	24.40	8.105
150	27.60	4.905
200	29.60	2.905

and from Figure 17,

$$C'_o = \frac{\Delta (\ln s - \phi')}{\Delta Z}$$

$$= \frac{\ln 22.505 - \ln 2.905}{200} = \frac{3.11373 - 1.06643}{200}$$

$$= \underline{.010236}$$

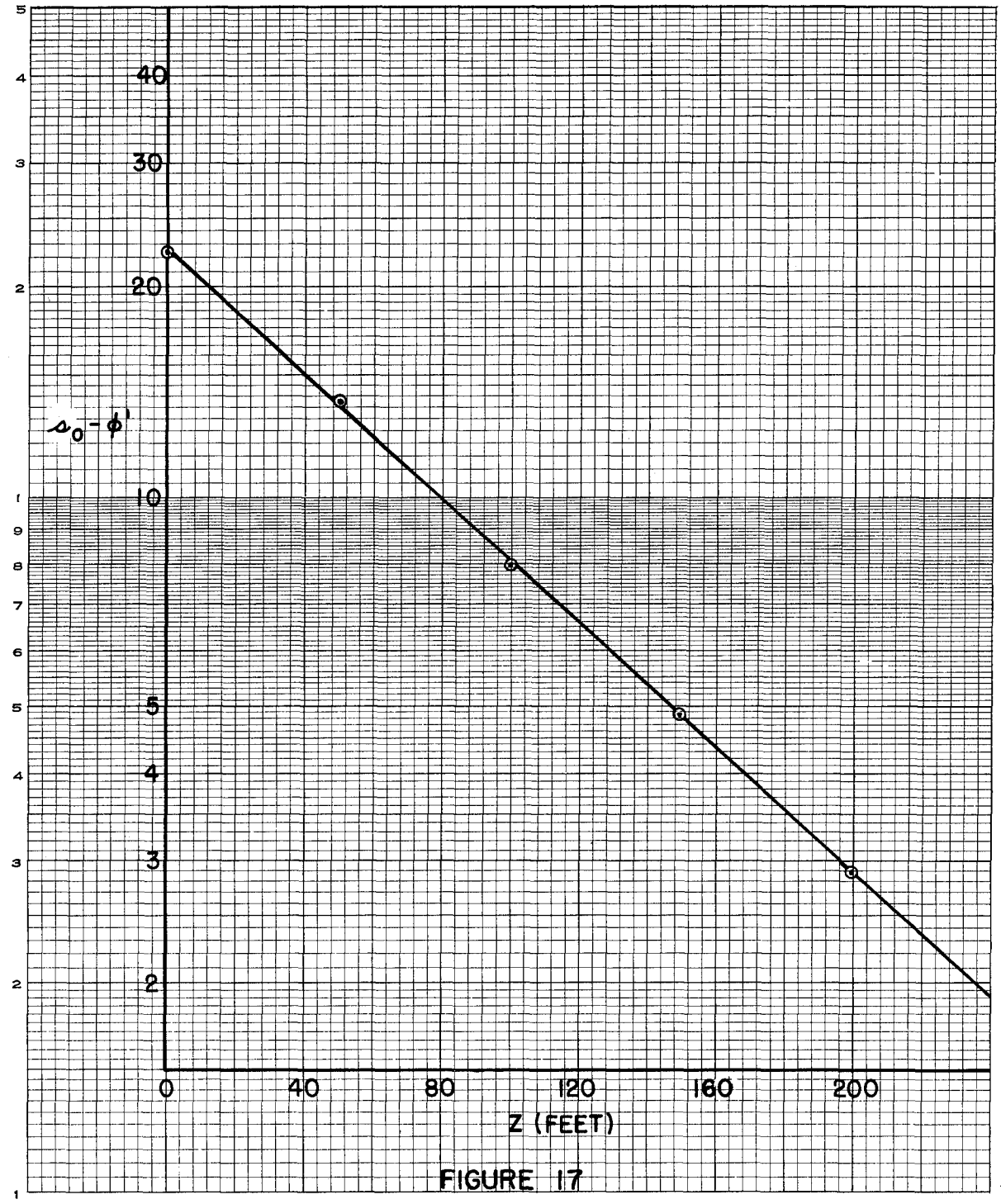

FIGURE 17

For Z = 0 from equation (15), an initial value of A may be obtained.

$$A_o = \frac{(s_o - \phi')}{C_{1_o}}$$

$$= \frac{22.505}{.010236} = \underline{2198.6^\circ}$$

When $Z = 0$, ϕ is equal to $B+A$ from which an initial value for B is obtained.

$$B_o = \phi_o - A_o$$

$$= 205.76 - 2198.61$$

$$= - \underline{1992.84}$$

These initial values for the constants are then substituted into equation (15) and values for ϕ are determined, which when compared with the measured values yield the residuals at all stations. (The 5th range station at $Z = 20$ ft. was taken as the origin).

By the Process of Differential Corrections, (see section "Method of Data Reduction" B, 1.) new values for the constants may be obtained.

TABLE X

Sta.	ΔB	Δs $Z_{x10^{-2}}$	ΔA $e^{-c_1 z}$	ΔC_1 $-zAe^{-c_1 z}$ $x10^{-4}$	$d\phi$
5	1	0	1	0	.0100
6	1	.096238	.90618	-1.917385	.8520
7	1	.206509	.80947	-3.675258	2.0337
8	1	.316856	.72301	-5.036797	.4826
9	1	.416701	.65276	-5.980344	- .2713
10	1	.495128	.60242	-6.557904	.2298
11	1	.576700	.55415	-7.026280	-1.3931
13	1	.735225	.47115	-7.616011	-4.7240
14	1	.856047	.41634	-7.835991	-5.8101
15	1	.975950	.36825	-7.901664	-8.2936
16	1	1.096611	.32547	-7.847147	-10.4756
17	1	1.146983	.30911	-7.795038	-12.9006
18	1	1.196543	.29382	-7.729616	-12.5386
19	1	1.245357	.27950	-7.652862	-11.7044
20	1	1.295909	.26541	-7.562058	-14.7953
21	1	1.656087	.18357	-6.683948	-20.1296
24	1	1.895676	.14365	-5.987121	-23.3452
25	1	1.977403	.13212	-5.743968	-23.5488
	18	16.185923	8.436380	-110.549392	-146.322100
		20.556000	5.028149	-112.251725	-215.882537
			5.134326	-44.089211	-34.171729
				763.887375	1036.121366
.899218		6.001327	-2.557996	-12.843722	-84.307071
.468688			1.180296	7.723962	34.407683
-6.141633				84.933581	137.464728
- .426238			.089981	2.249480	-1.527194
-2.140147				57.446128	-42.964797
24.999500				1.210253	-4.785710

ΔB -81.934704
Δs 12.390916 x 10^{-2}
ΔA 81.883242
ΔC_1 - 3.954305 x 10^{-4}

TABLE XI

Sta.	ΔB	Δs	ΔA	ΔC_1	
		z	$e^{-c_1 z}$	$-zAe^{-c_1 z}$	dØ
		10^{-2}		10^{-4}	
5	1	0	1	0	.0400
6	1	.096238	.90964	-1.996384	- .4999
7	1	.206509	.81610	-3.826605	.0039
8	1	.316856	.73211	-5.290130	-1.4690
9	1	.416701	.66360	-6.306075	-1.6768
10	1	.495128	.61431	-6.936386	.4210
11	1	.576700	.56691	-7.455766	-1.0870
13	1	.735225	.48504	-8.132535	-2.1645
14	1	.856047	.43066	-8.407373	-1.2416
15	1	.975950	.38275	-8.518207	-1.6392
16	1	1.096611	.33988	-8.499753	-1.6550
17	1	1.146983	.32344	-8.460166	-3.1825
18	1	1.196543	.30804	-8.405501	-1.9323
19	1	1.245357	.29359	-8.338028	.2344
20	1	1.295909	.27935	-8.255652	-2.4564
21	1	1.656087	.19598	-7.401556	-2.0667
24	1	1.895676	.15482	-6.692978	-2.1567
25	1	1.977403	.14285	-6.441746	-1.4262
	18	16.185923	8.639050	-119.364841	-25.265300
		20.556000	5.235000	-122.357940	-27.884490
			5.297827	- 48.685516	- 9.571296
				892.690541	190.743340
.899218		6.001327	-2.533389	-15.022926	-5.165477
.479947			1.151541	8.603281	2.554709
-6.631380				101.136922	23.199535
-.422138			.082101	2.261533	.374165
-2.503267				63.530527	10.268967
27.545742				1.234922	-.037686

ΔB -5.403122
Δ s 1.341582 x 10^{-2}
ΔA 5.397988
Δ C_1 .030517 x 10^{-4}

The new values now become

$B + \Delta B = -2074°$

$s + \Delta s = 32.63$

$A + \Delta A = 2280°$

$C_1 + \Delta C_1 = .009841$

The above process is repeated until the corrections become negligibly small, and the sum of the residuals squared reaches a minimum. (See Tables XI and XII.)

In the second application of the Differential Corrections, the corrections in C_1 and s were sufficiently small to make a third application unnecessary.

The final values are:

$B = 2079°$

$s = 32.64$ (°/ft.)

$A = 2285°$

$C_1 = .009838$

$C_2 = .321112$

TABLE XII

Sta	Residuals from Original Constants	Residuals from First Correction	Residuals from Second Correction
5	.0100	.0400	- .0800
6	.8520	- .4999	- .2066
7	2.0337	.0039	.5492
8	.4826	-1.4690	- .7373
9	- .2713	-1.6768	- 1.5083
10	.2298	- .4210	.5966
11	- 1.3931	-1.0870	.0042
13	- 4.7240	-2.1645	- .8776
14	- 5.8101	-1.2416	.1561
15	- 8.2936	-1.6392	- .1587
16	-10.4756	-1.6550	- .1152
17	-12.9006	-3.1825	- 1.6246
18	-12.5386	-1.9323	- .3598
19	-11.7044	- .2344	1.3491
20	-14.7953	-2.4564	- .8418
21	-20.1296	-2.0667	- .4749
24	-23.3452	-2.1567	- .5983
25	-23.5488	-1.4262	.0730
$\sum^2$	= 2426.04	49.1402	10.1249

The Probable Error is given by equation (39)

$$P.E._{\sigma_o} = .6745 \sqrt{\frac{10.1249}{14}} = \underline{\underline{.5736°}}$$

The Probable Errors of C_1 and s can be obtained from the equations:

$$P.E._{C_1} = \frac{P.E._{\sigma_o}}{W_{C_1}}$$

$$P.E._{s} = \frac{P.E._{\sigma_o}}{W_{s}}$$

Where W_{c_1} and W_s can be computed from the last Differential Correction Least Squares.

$$P.E._{C_1} = .00052 = .53\%$$

$$P.E._{s} = .0501 = .15\%$$

$$C_2 = C_1 s$$

$$P.E._{C_2} = \sqrt{(\%P.E._{C_1})^2 + (\%P.E._{s})^2}$$

APPENDIX C

VARIATION OF THE AERODYNAMIC DERIVATIVES WITH MACH NUMBER

The rolling motion of a rectangular fin stabilized missile at a Mach number of 1.7 and the associated aerodynamic coefficients namely C_{ℓ_δ}, C_{ℓ_p} and $\frac{p_s b}{2V}\Big/\delta$ are given in a previous paper.[1] Recently an initial study of the variation of these coefficients with Mach number has been undertaken for the same aerodynamic configuration (See Tables I and II) with the firing of three rounds near M = 2.5. Unfortunately only one of the three rounds has excellent statistical quality; however the results from the range firings and subsequent reduction for all three models are given herein.

As indicated in a previous paper[1] the equation expressing the rolling motion is

$$\phi = B + SZ + Ae^{-C_1 Z} \tag{1}$$

where

ϕ = roll angle

Z = distance along trajectory

A and B = constants (boundary condition)

S and C_1 = constants (model construction and aerodynamics)

The values of these constants and their Probable Error as obtained from the reduction procedure are given in Table III. The "fit" of the roll equation (equation 1) to the range data is given as a Probable Error in Table IV. Although the "fit" is very good since the estimated error in angle measurements is .7°, the values of the aerodynamic derivatives for models 5 and 6, as obtained from the constants by

$$C_{\ell_\delta} = \frac{2IC_2}{\rho b A_p n_\delta \delta} \tag{2}$$

$$C_{\ell_p} = \frac{4I}{\rho b^2 A_p n}\left(C_1 + \frac{K_R}{m}\right) \tag{3}$$

$$\frac{p_s b}{2V}\Big/\delta = \frac{sb}{2(57.3)\delta}\left[\frac{1}{1+\frac{K_R}{C_1 m}}\right] \tag{4}$$

are of relatively poor quality compared to model 7, as indicated by their Probable Errors (See Table V). The results on an individual round depend on the functioning of the range. A small number and/or a poor distribution of working stations will give data which although having an excellent "fit" may yield, as in this case, relatively poor aerodynamic derivatives.

[1] BRL Report No. 711

These new data are plotted in figures 17, 19, and 20 together with (1) the curve obtained from linearized theory as applying to this configuration and (2) the previous data on this configuration. In fairing a curve through these data an attempt was made to take into account the relative weights as obtained from the reciprocal of the Probable Error, which indicate that model 5 and 6 should be weighted approximately 1/4 that of model 7.

The results show that the experimental curve for C_{ℓ_p} at M = 1.7 deviates from linearized theory by 16% and that the deviation increases with increasing Mach number until at M = 2.7 the value is 22%. The experimental curve for C_{ℓ_δ} at M = 1.7 deviates by 7% and at M = 2.7 by 17%. The experimental curve for $\frac{p_{sb}}{2V}\Big/\delta$ deviates -11% at M = 1.7 approximately -5% at M = 2.7.

One source for this deviation may be the neglection of the thickness effect in the linearized theory, for if a comparison is made to the lift of an infinite-aspect-wing of such cross section (16% thickness wing wedge) computed from the exact theory using oblique shock equations, the result is an about 15% lower value for the linearized lift at M = 1.7 and about 22% at M = 2.6. Although this would tend to explain the variation of C_{ℓ_p} it sheds little light on C_{ℓ_δ} which not only deviates from theory by far less but with increasing Mach number departs more rapidly from theory than does C_{ℓ_p}. A brief discussion of these derivatives is given in the previous paper[1] but there is still no satisfactory explanation of the variation of these derivatives with Mach number.

TABLE I

Thick-Finned Roll Models

Round No.	Missile No.	Av. Angle of Cant in Two Tail Fins	Material	Moment of Inertia in Roll I (slugs - ft^2)	Mass of Missile M (slugs)
2125	5	1.9333°	Aluminum fuselage & bronze fins	1.266×10^{-5}	.012256
2324	6	2.1000°	"	1.263×10^{-5}	.012225
2322	7	4.4542°	"	1.243×10^{-5}	.012208

TABLE II

Thick-Finned Roll Models

Missile No.	Mach. No. at Beginning of Trajectory	Mach No. at End of Trajectory	Mach No. at Center of Data	Vel. of Sound in Range Atmosphere ft/sec	Air Density of Range Atmosphere slugs/ft^3
5	2.722	2.587	2.682	1125	2.342×10^{-3}
6	2.301	2.166	2.247	1132	2.309×10^{-3}
7	2.450	2.327	2.416	1132	2.311×10^{-3}

[1] BRL Report No. 711

TABLE III

Thick-Finned Roll Models

Model	5	6	7
P.E.	.7°	.3°	.6°

TABLE IV

Thick-Finned Roll Models

(yaw cards)

Model	5	6	7
A	918.12°	924.91	1930.38
B	-919.60°	-900.19	-1776.07
C_1	.012383	.012692	.012786
% Error	1.50	1.98	.36
s	14.173	15.777	33.579
% Error	.42	.87	.09
C_2	.175504	.200242	.429341
% Error	1.56	2.16	.37
K_R/m	1.836×10^{-4}	2.160×10^{-4}	1.864×10^{-4}
% Error	1.15	.14	.65
$\overline{\text{Yaw}^2}$	1.6880	1.5894	.0919
Number of Observations	14	14	19

TABLE V

Thick-Finned Roll Models

Model	5	6	7
Mach	2.682	2.247	2.416
(Theor.) C_{ℓ_p}	.3100	.3622	.3399
(Ex.) C_{ℓ_p}	.4014	.4258	.4242
P.E. %	1.48%	1.95%	.35%
Dev. from theory	29.5%	17.6%	24.8%
(Theor.) C_{ℓ_δ}	.4605	.5494	.5107
(Ex.) C_{ℓ_δ}	.5695	.6177	.6192
P.E.	1.56%	2.16%	.37%
Dev. from theory	23.7%	12.4%	21.2%
(Theor.) $\frac{Pb}{2V}$	.02506	.02780	.05839
(Ex.) $\frac{pb}{2V}$	.0236	.0261	.0559
P.E.	.43%	.88%	.09%
Dev. from theory	-5.83%	-6.11%	-4.26%

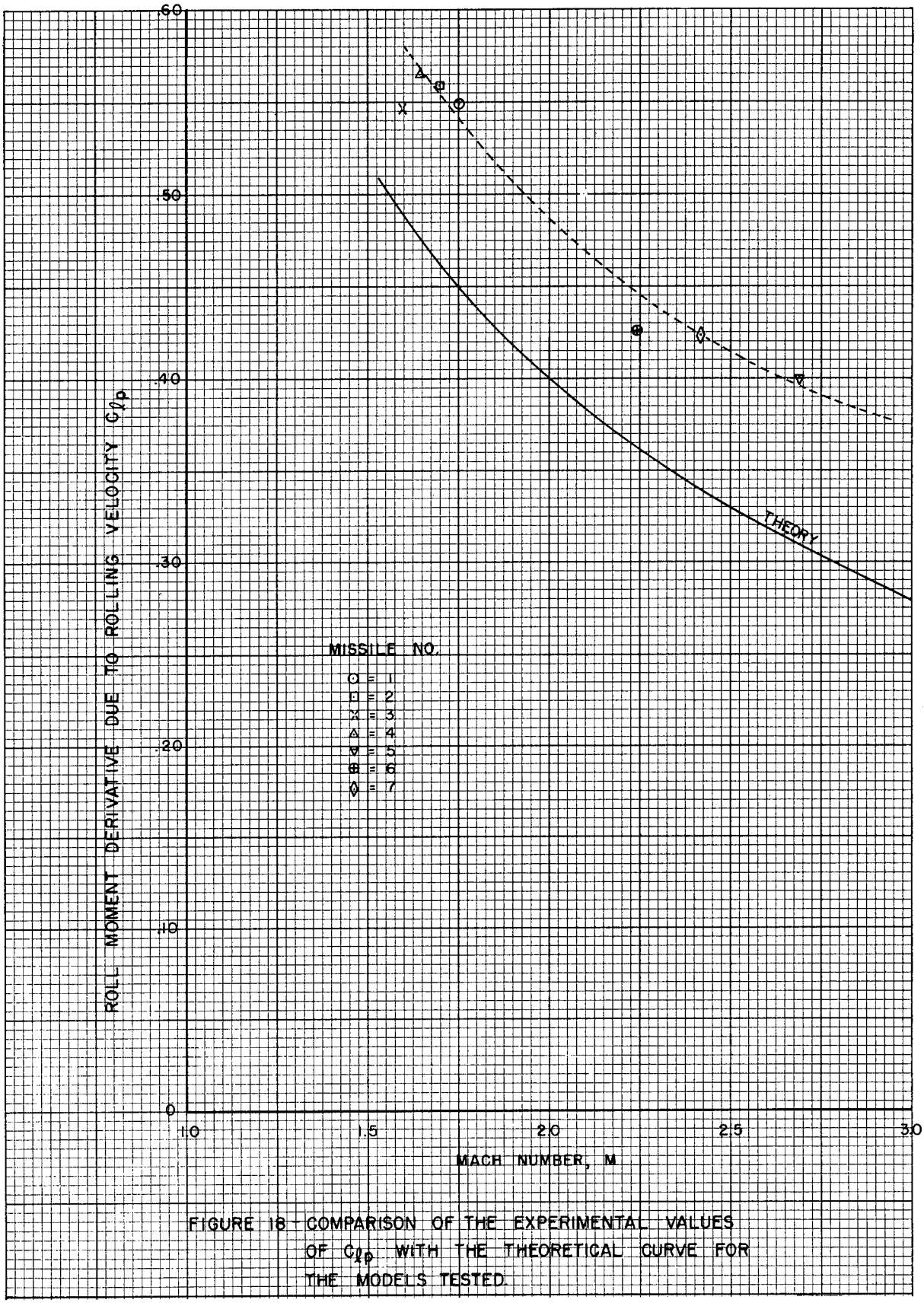

FIGURE 18 - COMPARISON OF THE EXPERIMENTAL VALUES OF C_{ℓ_p} WITH THE THEORETICAL CURVE FOR THE MODELS TESTED.

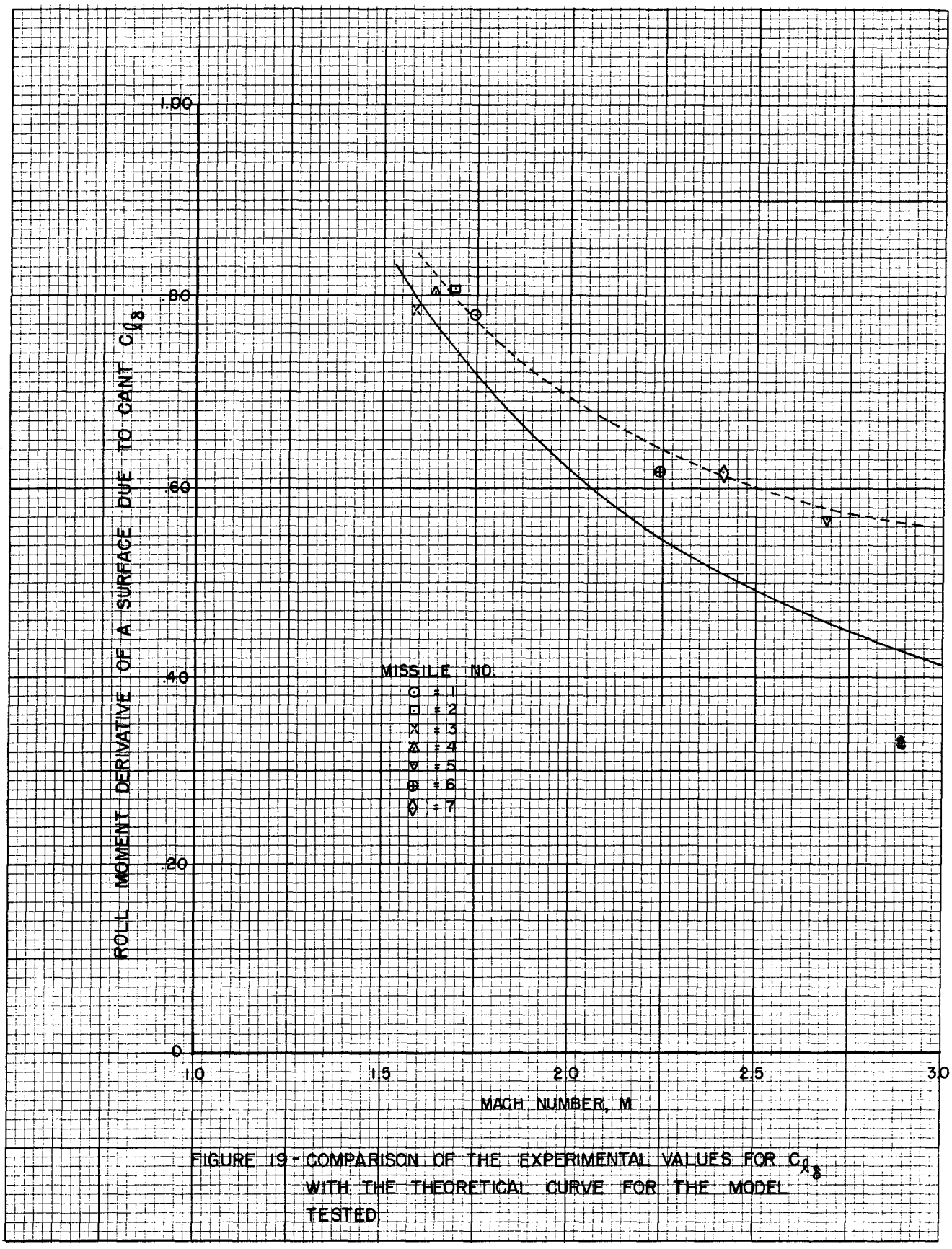

FIGURE 19 - COMPARISON OF THE EXPERIMENTAL VALUES FOR C_{l_δ} WITH THE THEORETICAL CURVE FOR THE MODEL TESTED

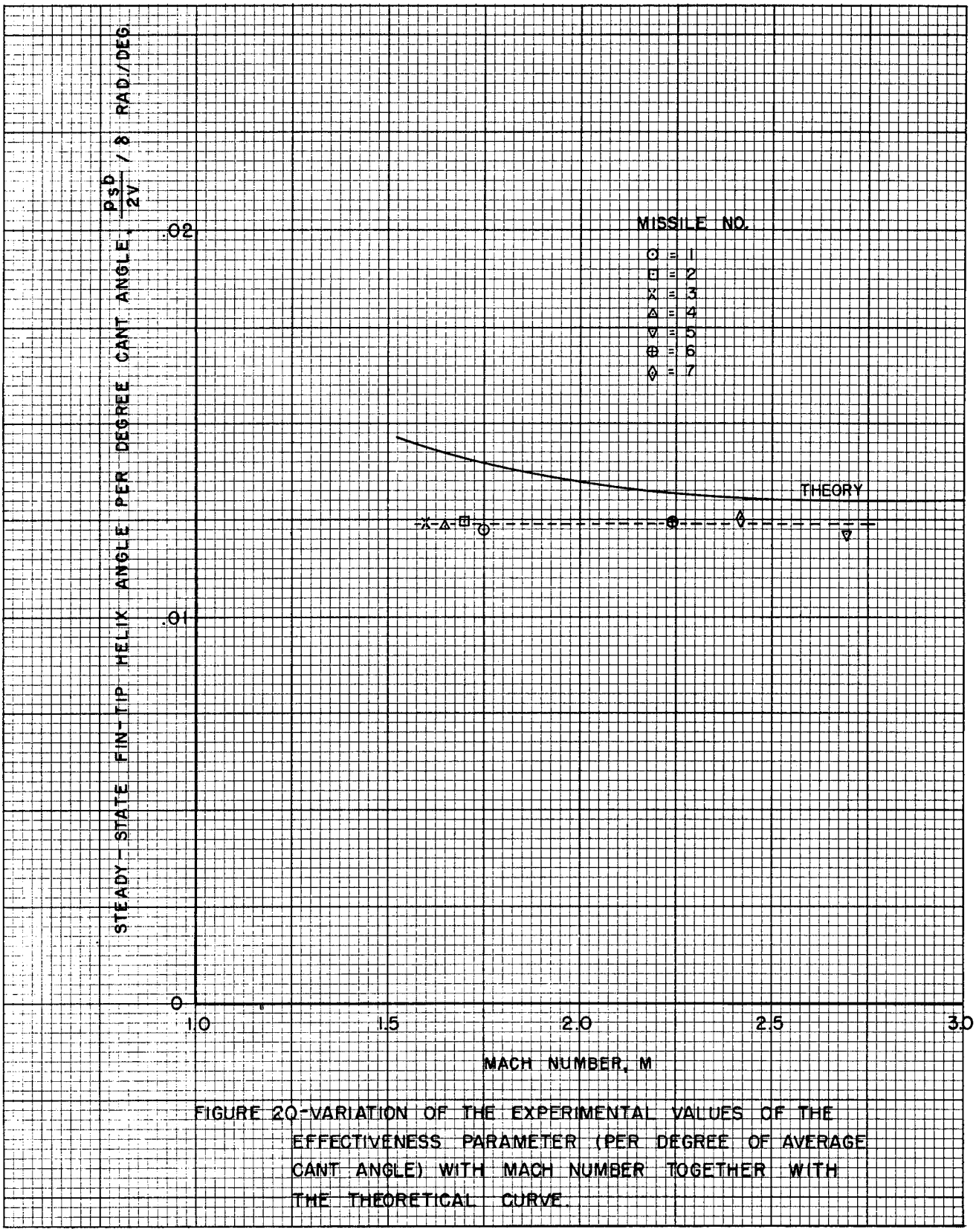

FIGURE 20-VARIATION OF THE EXPERIMENTAL VALUES OF THE EFFECTIVENESS PARAMETER (PER DEGREE OF AVERAGE CANT ANGLE) WITH MACH NUMBER TOGETHER WITH THE THEORETICAL CURVE.

DISTRIBUTION LIST

No. of Copies	
6	Chief of Ordnance Washington 25, D. C. ATTN: ORDTB-Bal Sec
10	British - send to ORDTB for distribution
4	Chief, Bureau of Ordnance Navy Department Washington 25, D. C. ATTN: Re3
1	Commanding Officer Naval Proving Ground Dahlgren, Virginia
2	Office of Naval Research Navy Department Washington 25, D. C. ATTN: Scientific Literature Branch (N482)
1	Dr. H. L. Dryden Director of Aeronautical Research National Advisory Committee for Aeronautics Washington 25, D. C.
1	Mr. P. L. Alger Consulting Engineer General Electric Company 1 River Road Schenectady, New York
1	Professor John von Neumann Department of Mathematics The Institute for Advanced Study Princeton, New Jersey
1	Professor Francis H. Clauser Department of Aeronautical Engineering The Johns Hopkins University Baltimore 18, Maryland
1	Professor Garrett Birkhoff Department of Mathematics Harvard University Cambridge, Massachusetts
1	Professor Edward J. McShane Department of Mathematics The Institute for Advanced Study Princeton, New Jersey
1	Mr. J. L. Kelly Department of Mathematics University of California Berkeley, California
1	Dr. L. H. Thomas Watson Laboratory 612 West 116th Street New York 27, New York
1	Professor David L. Webster Department of Physics Stanford University Stanford University, Calif.
1	Mr. A. E. Puckett Hughes Aircraft Company Florence Ave. at Teal St. Culver City, California
1	Professor Howard W. Emmons Graduate School of Engineering Harvard University Cambridge 38, Massachusetts
1	Professor L. S. G. Kovaszny Department of Aeronautical Engineering The Johns Hopkins University Baltimore 18, Maryland
1	Professor Z. Kopal Department of Electrical Engineering Room 20-C-231 Cambridge 39, Mass.
1	Dr. E. P. Hubble Mount Wilson Observatory Pasadena, California
1	Professor G. Kuerti 109 Pierce Hall Harvard University Cambridge, Mass.
1	Dr. D. P. Porter General Electric Co. 1 River Road Schenectady, N. Y.

FIELD PRINTING PLANT
THE ORDNANCE SCHOOL
ABERDEEN PROVING GROUND
MARYLAND